Measurement of jet radial profiles in Pb–Pb collisions at sNN=2.76 TeV

Physics Letters B 796 (2019) 204–219

Contents lists available at ScienceDirect

Physics Letters B

www.elsevier.com/locate/physletb

Measurement of jet radial profiles in Pb–Pb collisions at $\sqrt{s_{\mathrm{NN}}} = 2.76$ TeV

ALICE Collaboration *

ARTICLE INFO

Article history:
Received 6 May 2019
Received in revised form 2 July 2019
Accepted 8 July 2019
Available online 12 July 2019
Editor: L. Rolandi

ABSTRACT

The jet radial structure and particle transverse momentum (p_{T}) composition within jets are presented in centrality-selected Pb–Pb collisions at $\sqrt{s_{\mathrm{NN}}} = 2.76$ TeV. Track-based jets, which are also called charged jets, were reconstructed with a resolution parameter of $R = 0.3$ at midrapidity $|\eta_{\mathrm{ch\,jet}}| < 0.6$ for transverse momenta $p_{\mathrm{T,\,ch\,jet}} = 30$–$120$ GeV/c. Jet–hadron correlations in relative azimuth and pseudorapidity space $(\Delta\varphi, \Delta\eta)$ are measured to study the distribution of the associated particles around the jet axis for different $p_{\mathrm{T,assoc}}$-ranges between 1 and 20 GeV/c. The data in Pb–Pb collisions are compared to reference distributions for pp collisions, obtained using embedded PYTHIA simulations. The number of high-p_{T} associate particles ($4 < p_{\mathrm{T,assoc}} < 20$ GeV/c) in Pb–Pb collisions is found to be suppressed compared to the reference by 30 to 10%, depending on centrality. The radial particle distribution relative to the jet axis shows a moderate modification in Pb–Pb collisions with respect to PYTHIA. High-p_{T} associate particles are slightly more collimated in Pb–Pb collisions compared to the reference, while low-p_{T} associate particles tend to be broadened. The results, which are presented for the first time down to $p_{\mathrm{T,\,ch\,jet}} = 30$ GeV/c in Pb–Pb collisions, are compatible with both previous jet–hadron-related measurements from the CMS Collaboration and jet shape measurements from the ALICE Collaboration at higher p_{T}, and add further support for the established picture of in-medium parton energy loss.

1. Introduction

At energy densities above approximately 0.5 GeV/fm^3 and temperatures above approximately 160 MeV [1], Quantum Chromodynamics (QCD) calculations on the lattice predict the existence of a phase transition from normal nuclear matter to a new state of matter called the Quark–Gluon Plasma (QGP), where the partonic constituents, quarks and gluons, are no longer confined in hadrons. There is compelling evidence from observations reported by experiments at the Relativistic Heavy Ion Collider (RHIC) [2–5] and at the Large Hadron Collider (LHC) [6–17] that the QGP is created in nuclear collisions at high collision energies.

A unique way to characterize the properties of the QGP is to utilize jets as a probe of the medium. Hard scatterings are expected to occur early in the collision evolution, producing high transverse momentum (p_{T}) partons that propagate through the expanding medium and eventually fragment into jets of hadrons. High-p_{T} partons lose energy in interactions with the medium due to elastic scattering and induced gluon radiation [18,19]. Besides a reduction of the jet energy, this can result in a broadening of the transverse jet profile and a softening of the fragmentation [20].

Jet quenching has been observed at RHIC [21–34] and at the LHC [8,16,17,35–47], e.g. via inclusive yield and correlation measurements of high-p_{T} hadrons and reconstructed jets. These measurements provide insights into the mechanisms of parton energy loss in the medium and eventually into the medium itself.

More differential measurements of the jet modification in a medium, i.e. measurements of modifications of jet angular profile and particle composition, can provide complementary information to observables that focus on the overall yield change like nuclear modification factors. Measurements of correlated associated particle production relative to jets or high-p_{T} particles allow for a detailed measurement of the redistribution of quenched energy around the jet. An excess of low-p_{T} particles in and around the jet up to large distances, as well as a suppression of high-p_{T} particles, have been reported [17,48–50]. Two-particle correlations and jet–hadron correlations show an angular broadening of low-p_{T} particles below 3 GeV/c in heavy-ion collisions with respect to pp collisions [50]. For low-p_{T} two-particle correlations, measurements also indicate an asymmetry in the shape of the near-side jet peaks: they are broader in $\Delta\eta$ compared to $\Delta\varphi$ [48,49]. The variables $\Delta\eta$ and $\Delta\varphi$ are the distance in pseudorapidity η and azimuth φ relative to the near-side jet. At the same time, measurements of the radial moment of jets point to a general collimation of jets in Pb–Pb collisions [51].

* *E-mail address:* alice-publications@cern.ch.

https://doi.org/10.1016/j.physletb.2019.07.020

Using jets instead of high-p_{T} particles as a reference (trigger) to study angular correlations—as done in this analysis—should have the advantage that jet properties better reflect the initial parton energy. This analysis extends the study of jet–hadron correlations into a regime of low track-based jet $p_{\mathrm{T,\,ch\,jet}}$ not yet explored with these techniques at the LHC.

In this paper, we study the correlation of charged particles (associates) with the direction of reconstructed track-based jets (triggers) in the $\Delta\varphi$-$\Delta\eta$ plane in the same event. The jets are reconstructed using charged particles above a certain transverse momentum $p_{\mathrm{T,const}}$. The analysis focuses on two aspects of the modification of jets within the medium created in Pb–Pb collisions compared to a PYTHIA [52] reference. First, the overall modification of the associated particle yield and its jet-energy dependence is studied. Second, the modification of the radial distribution of associated particles with respect to the jet axis is studied by comparing the Pb–Pb results to the PYTHIA reference. Both aspects are analyzed in detail for several jet transverse momenta $p_{\mathrm{T,\,ch\,jet}}$ and low and high p_{T} of associated charged particles. PYTHIA is used as vacuum baseline, because the size of the pp dataset at $\sqrt{s} = 2.76$ TeV is insufficient for this analysis.

The paper is structured as follows. In Sec. 2, details on the detector and general data reconstruction will be given. The correlation analysis, which serves as basis for this paper, is presented in Sec. 3. Subsequently, jet reconstruction will be described in Sec. 4, followed by a discussion on the embedded PYTHIA reference in Sec. 5. Before the results will be presented in Sec. 8, the observables are introduced in Sec. 6 and systematic uncertainties are discussed in Sec. 7. A summary concludes the paper in Sec. 9.

2. Experimental setup

For a complete description of the ALICE detector and its performance see Refs. [53] and [54], respectively.

The data were recorded in 2011 for Pb–Pb collisions at $\sqrt{s_{\mathrm{NN}}} = 2.76$ TeV using a set of centrality triggers based on the hit multiplicity measured by the V0 detector, which consists of segmented scintillators covering the full azimuth over $2.8 < \eta < 5.1$ (V0A) and $-3.7 < \eta < -1.7$ (V0C). Events were selected with V0 multiplicities corresponding to the 0–50% most central events using the centrality determination as described in Ref. [55]. The accepted events, reconstructed as described in Ref. [56], were required to have a primary reconstructed vertex within 10 cm of the center of the detector along the beam axis. For this analysis, a total of 12M events were used.

The analysis presented here relies mainly on the central ALICE tracking systems, which are located inside a large solenoidal magnet with a field strength of 0.5 T. They consist of the Inner Tracking System (ITS), a high-precision six-layer cylindrical silicon detector system with the inner layer at a radius of 3.9 cm and the outer layer at 43 cm from the beam axis, and the Time Projection Chamber (TPC) with a radial extent of 85–247 cm, which provides up to 159 independent space points per track.

To ensure a good track-momentum resolution for jet reconstruction, all reconstructed tracks were required to have at least three hits in the ITS. For tracks without any hit in the Silicon Pixel Detector (SPD), which provides the two innermost layers of the ITS, the location of the primary vertex was used in addition to the hits in the TPC and ITS. This improves the track-momentum resolution and reduces the azimuthal dependence of the track reconstruction efficiency due to the non-uniform SPD response. Accepted tracks were required to be measured with $0.15 < p_{\mathrm{T}} < 100$ GeV/c in $|\eta| < 0.9$, and to have at least 70 TPC space-points and no less than 80% of the geometrically findable space-points in the TPC.

The single-track tracking efficiency was estimated from the detector response of HIJING [57] events reconstructed to detector level using GEANT3 [58] for the particle transport. In the 0–10% centrality class, it is about 56% at 0.15 GeV/c, about 83% at 1.5 GeV/c and then decreases to 81% at 3 GeV/c, after which it increases and levels off to about 83% at above 6.5 GeV/c. For the 10–30% most central collisions, the tracking efficiency follows a similar p_{T}-dependence pattern, with absolute values of the efficiency that are 1 to 2% higher compared to the 0–10% most central collisions. The momentum resolution, which was estimated on a track-by-track basis using the covariance matrix of the track fit, is about 1% at 1 GeV/c and about 3% at 50 GeV/c. The contamination by secondary particles [59] produced in particle-material interactions, conversions, and weak-decay products of long-lived particles is on the level of few percent.

3. Correlation analysis

The two-dimensional associated per-trigger yield $Y(\Delta\varphi, \Delta\eta)$ measures the distribution of particles relative to the jet axes in bins of $\Delta\varphi$, $\Delta\eta$, event centrality, and trigger and associate transverse momenta $p_{\mathrm{T,\,assoc}}$ [60]. This distribution serves as the basis of the analysis and is formed using so-called same and mixed event correlations. Correlations from the *same event* are the actual correlations of trigger jets and associated particles, calculated for each selected event. In the mixed event technique, jets are correlated with particles from a pool containing tracks from different events with similar trigger jet p_{T}, vertex z, and centralities. For vertex z, there are six bins in this pool, whose boundaries are given by $(-10, -5, -2, 0, 2, 5, 10)$ in cm. The boundaries for the centrality percentile binning are given by $(0, 1, 2, 3, 4, 5, 10, 20, 30, 40, 50)$.

The mixed-event-corrected associated per-trigger yield for given jet p_{T}-range, associate p_{T}-range, and centrality selection is defined as

$$Y(\Delta\varphi, \Delta\eta) = \frac{1}{N_{\mathrm{trig}}} \frac{\mathrm{d}^2 N_{\mathrm{assoc}}}{\mathrm{d}\Delta\eta \mathrm{d}\Delta\varphi} = \frac{1}{N_{\mathrm{trig}}} \sum_{\mathrm{cent},z} \left(\frac{\mathrm{d}^2 N_{\mathrm{same}}}{\mathrm{d}\Delta\eta \mathrm{d}\Delta\varphi} \Big/ \alpha \frac{\mathrm{d}^2 N_{\mathrm{mixed}}}{\mathrm{d}\Delta\eta \mathrm{d}\Delta\varphi} \right), \quad (1)$$

where the ratios in the sum are formed differentially in bins of centrality and vertex z.

The factor α in Eq. (1) is chosen such that the mixed-event correlations are normalized to unity in the region $|\Delta\eta| < 0.2$, $|\Delta\varphi| < 0.2$ around the near-side jet peak where the efficiency for pairs of parallel jets and associates is largest. The contribution of the statistical uncertainty of this normalization to the total statistical uncertainty is negligible. The finite tracking efficiency and the contamination by secondaries (see Sec. 2) are taken into account and a correction has been performed for associated tracks differentially in η, p_{T}, centrality, and vertex z for same and mixed event correlations in Eq. (1). The efficiency maps were created using Monte Carlo simulations for the same track definition and detector conditions. However, this correction turns out to be negligible for all observables except for the absolute jet-associated yields, because its effect mostly cancels in the used relative observables, which will be defined in Sec. 6.

In addition to the correction for detector inhomogeneities and acceptance effects, the correlation also needs to be corrected for background. The underlying background for the chosen observables mainly consists of the uncorrelated particle background baseline from soft processes and the flow modulation in the correlation function. The background was found to be independent of $\Delta\eta$

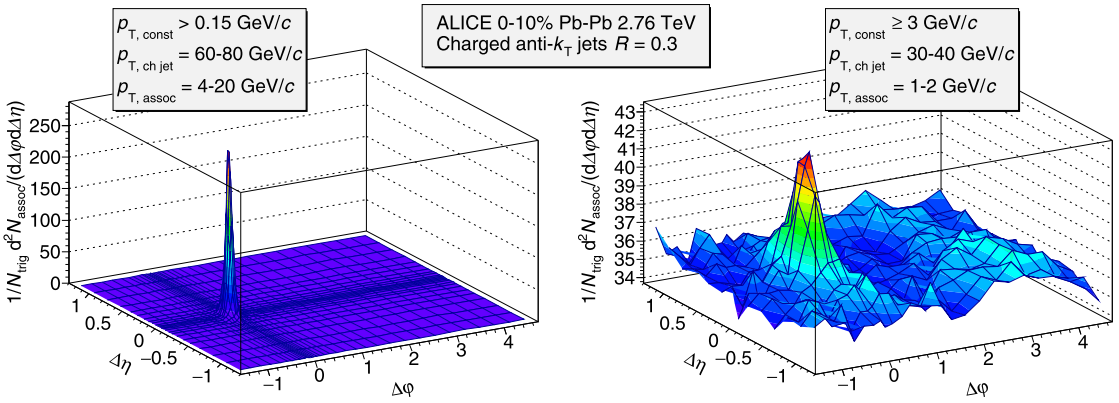

Fig. 1. Illustration of per-trigger yields for the two different jet definitions (further discussed below): high-p_T associates of jets with $p_{T,\,const} \geq 0.15$ GeV/c and $p_{T,\,ch\,jet} = 60$–80 GeV/c (left) and low-p_T associates of jets with $p_{T,\,const} \geq 3.0$ GeV/c and $p_{T,\,ch\,jet} = 30$–40 GeV/c (right). No background subtraction was applied.

within $|\eta| < 0.9$ [61] and is therefore estimated as a function of $\Delta\varphi$ for the whole $\Delta\eta$-range as $B(\Delta\varphi)$. To avoid including parts of the jet signal, $B(\Delta\varphi)$ is calculated in $1.0 < |\Delta\eta| < 1.4$, where the contribution from the jet is expected to be small, based on measurements in pp collisions.

The background is directly subtracted from the correlation function. The background-corrected per-trigger yield serves as a basis for all subsequent measurements. It is defined as

$$Y_{\mathrm{corr}}(\Delta\varphi, \Delta\eta) = Y(\Delta\varphi, \Delta\eta) - B(\Delta\varphi). \tag{2}$$

To illustrate the impact of the background on the per-trigger yields, the uncorrected per-trigger yields can be found in Fig. 1 for high- and low-p_T associates. The background is nearly negligible for high-p_T associates and it is sizeable for low-p_T associates. In the illustrated example for low-p_T associates, the signal to signal+background ratio, i.e. the percentage of the signal in the measured observable, is roughly 0.1 within a radius of $r < 0.3$ around the near-side jet peak. Note also that the background correction removes all $\Delta\eta$-independent correlations, including the away-side ridge which is not investigated in the presented analysis.

4. Jet reconstruction

The measurement of jets in heavy-ion collisions is challenging since a single event can contain multiple, possibly overlapping, jets from independent hard nucleon–nucleon scatterings. In addition, low transverse momentum particles originating from soft processes lead to a fluctuating background which strongly influences the jet reconstruction. The relative effect is largest for low-p_T jets and most central events. Consequently, jet reconstruction in heavy-ion collisions requires a robust jet definition, and a procedure to correct for the presence of the large background [62].

Jets were reconstructed using the anti-k_T or the k_T algorithms [63] in the FastJet package [64] with a resolution parameter of $R = 0.3$. Only those jets whose axis was reconstructed within $|\eta| < 0.6$ were kept in the analysis to assure the nominal jet cone is fully contained within the track acceptance of $|\eta| < 0.9$. This limits the effect of the acceptance boundaries on the measured jet spectrum. Jets reconstructed by the anti-k_T algorithm were used to quantify signal jets, while jets reconstructed by the k_T algorithm were used to quantify the contribution from the underlying event [65].

Two different jet definitions are used in this analysis: for measurements at high associate-p_T, jets are measured with a constituent cut $p_{T,\mathrm{const}} \geq 0.15$ GeV/c, measurements at low associate-p_T are performed for jets measured with a constituent cut $p_{T,\mathrm{const}} \geq 3.0$ GeV/c. Jets with $p_{T,\mathrm{const}} \geq 0.15$ GeV/c are reconstructed using all charged particles available for jet reconstruction and, thus, the fragmentation bias is as small as possible. This bias is caused by only including certain particles of the jet and could lead to a sample of harder fragmenting jets when leaving out particles at low p_T. On the other hand, using all charged particles available for jet reconstruction also includes particles in the correlation analysis which were already used in the jet finding process. The jet finding algorithm selects regions in momentum space with large energy flow. This implies that the distribution of charged particles inside the jet is biased. For example, the radial distribution of particles with respect to the jet axis will show a small depletion at distances just outside the jet cone radius R. This particularly affects the shape of the jet, i.e. how the constituents are distributed relative to the jet axis, leading to an autocorrelation bias.

Therefore, the jets themselves and in particular their shapes are intimately connected to the jet definition. For high-p_T associates, the autocorrelation bias cannot be avoided and has to be accepted as a part of the jet definition.

Low-p_T associates are broadly distributed up to large distances relative to the jet. Since the jet finding algorithm clusters the jets roughly into cones with a nominal radius of $R = 0.3$, it strongly affects the shape of the jet. When measuring properties of low-p_T associates, we avoid the autocorrelation bias by adapting the jet definition: Trigger jets and associates can be decoupled by using jets with constituents *above* a certain threshold and associates *below* the threshold. Therefore, for measurements at low associate-p_T, jets are reconstructed with $p_{T,\mathrm{const}} \geq 3$ GeV/c. Using a geometrical matching procedure that is performed on two collections of the differently defined jets which are reconstructed in each event it was checked that the jet axes for both jet definitions do not strongly change. For instance, for jets with $p_{T,\mathrm{const}} \geq 3$ GeV/c and $p_{T,\,ch\,jet} > 30$ GeV/c the mean and standard deviation of the matched jet distance distribution are approximately given by 0.016 and 0.014, respectively. However, it must be emphasized that these jet definitions select two different jet samples and that the autocorrelation bias was avoided here at the expense of a possible fragmentation bias.

The transverse momentum of reconstructed jets including constituents as low as 0.15 GeV/c is affected by the contribution from the underlying event. In order to suppress the contribution of such background to the measurement of the jet momentum, we followed the approach described in Refs. [65,66], which addresses the average additive contribution to the jet momentum on a jet-by-jet basis. The underlying background momentum density ρ was estimated event-by-event using the median of $p_{T,\,\mathrm{jet}}^{\mathrm{raw}}/A_{\mathrm{jet}}$, where $p_{T,\,\mathrm{jet}}^{\mathrm{raw}}$

Table 1
True jet populations $p_{\mathrm{T,\,true}}$ in GeV/c corresponding to given $p_{\mathrm{T,\,ch\,jet}}$-ranges for different event centrality classes. The ranges are given such that they contain at least 68% of the jet population. The most probable values of the distributions are given in parentheses.

$p_{\mathrm{T,\,const}}$-cut	0.15 GeV/c			3 GeV/c	
$p_{\mathrm{T,\,ch\,jet}}$ (GeV/c)	40–60	60–80	80–120	30–40	40–60
0–5%	11–87 (44)	22–111 (64)	49–144 (94)	7–59 (32)	21–88 (46)
5–10%	11–86 (46)	24–112 (66)	52–146 (94)	8–61 (32)	22–89 (46)
0–10%	11–86 (46)	25–113 (68)	54–147 (94)	10–63 (32)	24–91 (48)
10–30%	13–86 (50)	33–117 (70)	63–149 (98)	15–69 (32)	30–94 (48)
30–50%	25–91 (52)	47–118 (82)	75–147 (98)	23–73 (32)	36–95 (52)

is the uncorrected jet transverse momentum and A_{jet} is the area of jets reconstructed with the k_{T} algorithm.

The average raw background momentum density $\langle\rho\rangle$ decreases towards more peripheral collisions. It is $\langle\rho\rangle \approx 110$, 65, and 25 GeV/$c$ in the 0–10%, 10–30%, and 30–50% most central Pb–Pb collisions, respectively. The background momentum density is a detector-level quantity that depends on the tracking efficiency and track definition. For signal jets reconstructed with the anti-k_{T} algorithm and constituents above 0.15 GeV/c, the background density scaled by the area of the reconstructed signal jet was subtracted from the raw reconstructed transverse momentum ($p_{\mathrm{T,\,jet}}^{\mathrm{raw}}$) of the signal jet according to $p_{\mathrm{T,\,ch\,jet}} = p_{\mathrm{T,\,jet}}^{\mathrm{raw}} - \rho \cdot A_{\mathrm{jet}}$.

Due to region-to-region variations of the background, the background-corrected jet transverse momenta are affected by residual fluctuations. To give an estimate for these fluctuations for the jet definition used, cones with radius $R = 0.3$ are randomly placed in each event. In these cones, the track momenta are summed and the background is subtracted to calculate δp_{T}:

$$\delta p_{\mathrm{T}} = \sum_{\mathrm{cone}} p_{\mathrm{T,\,track}} - \rho \cdot A, \tag{3}$$

where A is the area of the cone.

For the 0–10%, 10–30%, and 30–50% most central collisions, the standard deviation of the δp_{T}-distribution as a measure for the magnitude of the fluctuations has been evaluated to 6.7, 5.1, and 3.3 GeV/c, respectively. Since the δp_{T}-distribution also contains the jet signal, the standard deviation of the full distribution is impacted by it. A lower limit of these fluctuations is given by performing a Gaussian fit of the left-hand side of the δp_{T}-distribution. The Gaussian widths were evaluated to 5.5, 4.0, and 2.3 GeV/c for the 0–10%, 10–30%, and 30–50% most central collisions. The sample of jets that only uses constituents above 3 GeV/c is not corrected for the underlying event as the constituent cut already strongly suppresses the contribution from the background such that it is negligible.

In addition to background fluctuations, also the finite detector resolution and single particle efficiency influence the measurement. To quantify both effects, the ratio of reconstructed jet momentum $p_{\mathrm{T,\,rec}}$ and true jet momentum $p_{\mathrm{T,\,true}}$ was calculated taking into account the detector resolution by using a response matrix and background fluctuations given by the δp_{T} distributions. The response matrix was created from Monte Carlo simulations for which the true jet momentum is known by geometrically matching particle-level PYTHIA jets with the corresponding detector-level jets reconstructed using a full detector model in GEANT3. More detailed studies have been performed for jets on the same dataset in Ref. [66].

There are two effects contributing to the jet momentum resolution: detector effects and underlying event fluctuations. The detector effects lead to a jet momentum response that is peaked at $p_{\mathrm{T,\,rec}} = p_{\mathrm{T,\,true}}$, but has a tail to lower values of detector level momentum due to tracking inefficiency. The tracking efficiency changes by only a few percent from peripheral to central events. Background fluctuations produce an approximately Gaussian response, with a width that depends strongly on centrality. The combined effect leads to a standard deviation in the jet momentum resolution of 30% (20%) for jets with $p_{\mathrm{T,\,ch\,jet}} = 30$ GeV/c and 27% (27%) for jets with $p_{\mathrm{T,\,ch\,jet}} = 120$ GeV/c for the 0–10% (10–30 and 30–50%) most central events.

It should be emphasized that $p_{\mathrm{T,\,ch\,jet}}$ refers to the jet transverse momentum at detector level, corrected for background only. Since within-event fluctuations of the background are not corrected for, the mean of the given $p_{\mathrm{T,\,ch\,jet}}$-range is slightly higher than that of the underlying *true* p_{T} distribution for more central collisions where fluctuations are dominant. Hence, due to the steeply-falling jet spectrum, fluctuations lead to a shift of the spectrum to larger values. For more peripheral collisions where detector effects are dominant, there is the opposite effect, i.e. the spectrum is shifted to smaller values. The fraction of purely combinatorial jets in the momentum ranges used in the analysis was found to be negligible.

To give a rough estimate of the true jet populations for a given reconstructed jet momentum range, projections of the response matrices, introduced above, are used [67]. For measured $p_{\mathrm{T,\,ch\,jet}}$-distributions, approximate ranges are given in Table 1 as a measure for the true jet momentum distributions. The true populations are defined as the smallest possible ranges around the $p_{\mathrm{T,\,ch\,jet}}$-range in which at least 68% of the jet population can be found.

5. Construction of PYTHIA baseline

In this analysis, reconstructed detector-level PYTHIA-jets serve as vacuum baseline, because the size of the pp dataset at $\sqrt{s} = 2.76$ TeV is insufficient for this purpose.

To account for the fluctuations of the underlying event in Pb–Pb collisions, PYTHIA jets embedded in real Pb–Pb collisions are used as a reference. Jets reconstructed in this reference dataset still show the same baseline jet properties but also include the effect of background fluctuations from the Pb–Pb event. To create this reference dataset, the following procedure is applied. Events are simulated with PYTHIA6 (Perugia-0 [68], version 6.421) followed by transport in the detector using GEANT3 and full response simulation and reconstruction simulating the same detector conditions as in the Pb–Pb dataset. The reconstructed tracks are embedded into Pb–Pb events, i.e. they are combined with tracks from Pb–Pb events. In order to simulate the same conditions as in Pb–Pb, the tracking efficiency in pp is decreased to the level expected in Pb–Pb. Since the tracking efficiency in pp is higher than in Pb–Pb, 2% of the PYTHIA tracks are randomly discarded before they are embedded [54]. Jet finding algorithms are applied to the PYTHIA event and also to the combined PYTHIA + Pb–Pb event. Jets found in the combined event are only accepted for the reference dataset if they can be matched geometrically with those in the PYTHIA event. A matched embedded jet needs to be less than $R = 0.3$ away from a PYTHIA jet.

Due to the very high particle occupancy of the Pb–Pb collision system, the probability to reconstruct a PYTHIA jet in the embedded event is much lower than the probability to reconstruct a jet of same momentum by overlapping a jet that already existed in the Pb–Pb event, even after applying a geometrical matching procedure. Therefore, without any further intervention, the embedded jet sample would consist mostly of Pb–Pb-jets overlapping low-p_{T} PYTHIA jets.

Two approaches have been tested which ensure that the jet sample shows Pb–Pb-event-like fluctuations of a PYTHIA jet, and not jets from the Pb–Pb event. The analysis baseline technique uses a cut on the fraction of the jet p_{T} that originates from the matched jet in PYTHIA. The applied cut values are motivated by the underlying true jet distribution that shows two separated populations: jets mostly consisting of particles from PYTHIA or from Pb–Pb. The cut value was chosen to achieve the best separation of the two distributions. In the 0–10% most central collisions, it is required that at least 20% of the jet constituents' p_{T} originate from the PYTHIA jet. For more peripheral collisions, this fraction is increased to 25%. For jets with $p_{\mathrm{T,\,const}} \geq 3$ GeV/c, which were measured down to 30 GeV/c, a cut of 50% is applied. However, this procedure might impose a bias on the implicitly accepted background fluctuations. Therefore, variations around these nominal values were considered for the evaluation of systematic uncertainties. Alternatively, a jet veto technique has been used: an embedded jet is not accepted if it overlaps with an already existing jet of sizeable transverse momentum $p_{\mathrm{T,\,ch\,jet}}$ in the Pb–Pb event. Several veto cut values between 15 and 40 GeV/c were tested. Eventually, it turns out that both approaches yield very similar results. The reconstructed jets which survive the MC percentage cut serve as an input to the next analysis steps which are the same as in the data analysis.

6. Observables

In this analysis, two features of particle jets are probed in Pb–Pb collisions: changes in the particle p_{T} composition of jets and their radial distribution relative to the jet axis.

To probe relative changes in the charged particle p_{T} composition of jets in a surrounding cone with $R = 0.3$, the jet-associated yield ratio is measured. The ratio is formed from the integrated jet-associated per-trigger yields Y_{PbPb} and Y_{emb} which represent the integrals of the per-trigger yield in the jet cone for a given $p_{\mathrm{T,\,assoc}}$-range as introduced in Eq. (2). Technically, the integral is the sum over the entries of all $(\Delta\eta, \Delta\varphi)$-bins whose center is within distances of up to $R = 0.3$ around the jet axis in the background-corrected per-trigger yield histogram.

The jet-associated yield ratio is defined by $R_{\mathrm{Y}} = Y_{\mathrm{PbPb}}/Y_{\mathrm{emb}}$. It directly compares integrated jet-associated per-trigger yields in Pb–Pb to the same yields for embedded PYTHIA jets. An enhancement or suppression in associated yields is directly seen as a deviation from unity in the ratio.

The relative radial particle distribution around the jet is directly derived from the jet-associated yields. It shows the relative distribution of particle yields inside the jet cone. Thus, it is a measure for the broadening or collimation of constituents with certain momenta in or around the jet cone. As for the jet-associated yield ratio, this measurement is performed for high- and low-p_{T} jet-associated yields. The radial shape is normalized to represent a probability distribution. It is defined in bins of $r = \sqrt{\Delta\eta^2 + \Delta\varphi^2}$, the distance to the jet axis, to exploit the radial symmetry of the jet peak. In Refs. [48,49], an asymmetric broadening of the near-side jet peak is observed in two-particle correlations. It is strongest for low associate and trigger momenta and vanishes for higher momenta. Therefore, in the analysis presented here, the influence of this asymmetry on jet–hadron correlations was tested to check the radial symmetry of the jet peak. Even for the lowest accessible jet and associated track momenta, no jet peak asymmetry was observed. Measurements in $\Delta\eta$ and $\Delta\varphi$ lead to the same conclusions within statistical precision, which justifies the presentation of the jet radial shape in bins of r. The correlation function which is used to obtain the shape is originally binned in η and φ. The binning was chosen fine enough to avoid significant binning effects.

For a given centrality-bin, and trigger and associate p_{T}, it is defined by the following formula:

$$S(r_{\mathrm{min}}, r_{\mathrm{max}}) = \frac{1}{A} \int_{r_{\mathrm{min}}}^{r_{\mathrm{max}}} Y_{\mathrm{corr}}(r)\mathrm{d}r, \tag{4}$$

where $Y_{\mathrm{corr}}(r)$ represents the background-corrected per-trigger yield, r_{min} and r_{max} the bin edges, and $A = \int_0^{r_{\mathrm{range}}} Y_{\mathrm{corr}}(r)\mathrm{d}r$ the integral for the self-normalization of the radial shape. The upper limit in the integral used for the self-normalization is chosen to reflect the different ranges of the shown radial shape and is $r_{\mathrm{range}} = 0.3$ for the jets with $p_{\mathrm{T,\,const}} \geq 0.15$ GeV/c and $r_{\mathrm{range}} = 0.9$ for jets with $p_{\mathrm{T,\,const}} \geq 3$ GeV/c. The statistical uncertainty is calculated taking into account the self-normalization.

7. Systematic uncertainties

Several sources of systematic uncertainties contribute to the full uncertainty of the measurement and the evaluated individual uncertainties are combined using a quadratic sum, assuming they are uncorrelated. Uncertainties for the following analysis aspects have been taken into account: the non-jet-related background correction technique, the mixed-event correction, the selection of embedded jets, the tracking efficiency, and the impact of using a PYTHIA reference instead of a measured reference in pp at the same energy. The uncertainties are partly correlated point-to-point. The discussed uncertainties are summarized in Tables 2–4.

To correct for the non-jet-correlated background in the correlation function, the background is evaluated on the sidebands and subtracted in $\Delta\varphi$, as described in Sec. 3. Different underlying background methods for the correlation functions have been tested: for systematic uncertainties, the definition of the sideband range was varied to $1.1 < |\Delta\eta| < 1.3$ instead of $1.0 < |\Delta\eta| < 1.4$. In addition, a simpler method that approximates the background by a constant baseline ($B(\Delta\varphi = \mathrm{const})$) has been used.

The mixed-event acceptance/inhomogeneity correction is a small correction. Two variations are considered for systematic uncertainties. First, the mixed-event correction is calculated inclusively for all $\Delta\varphi$. Second, the normalization of the mixed-event correlations is performed for $|\Delta\eta| < 0.3$ and full $|\Delta\varphi|$ instead of using the plateau in $|\Delta\eta| < 0.2$ and $|\Delta\varphi| < 0.2$.

In the embedding, a cut motivated by studying the underlying true jet distributions is applied on the fraction of jet p_{T} originating from the PYTHIA event, as described in Sec. 5. Instead of cutting at 20% for 0–10% centrality, and 25% for other centralities, the cut is varied to 15% and 25% for 0–10% centrality, and to 20% and 30% for other centralities. As described above, for jets with $p_{\mathrm{T,\,const}} \geq 3$ GeV/c a baseline cut value of 50% is used. For systematic variation, the cut is performed at 15% and 60% for 0–10% centrality, 20% and 60% for other centralities.

The detector has a finite single track reconstruction efficiency, which is only known with finite precision. Since all observables are corrected for the tracking efficiency, they are all directly affected by its uncertainty. Detailed studies of the tracking efficiency uncertainty have been performed to evaluate the size of its systematic uncertainty [54,66]. The studies indicate that the (absolute) uncertainty is 4% for Pb–Pb collisions, mainly due to an imperfect

Table 2
Table of systematic uncertainties for jet-associated yields in Pb–Pb, embedded PYTHIA, and their ratio for high-p_{T} associates (4–20 GeV/c) and low-p_{T} associates (1–2 GeV/c) and for the 0–10% most central collisions. Uncertainties are given as relative uncertainties in percentages.

$p_{\mathrm{T,\,assoc}}$ (GeV/c)	Observable	4–20			1–2	
$p_{\mathrm{T,\,ch\,jet}}$ (GeV/c)		40–60	60–80	80–120	30–40	40–60
Background (%)	Pb–Pb	0.3–0.6	0.7–1.5	1.5–2.0	6.9	8.0
	Embedded	0.3–0.7	0.7–1.0	1.0–1.1	6.8	6.7
	Ratio	0.4–0.7	0.1–0.7	0.4–1.6	6.9	9.6
Mixed event correction (%)	Pb–Pb	0.2	0.3	0.5	0.2	0.2
	Embedded	0.7	0.4	0.4	0.1	<0.1
	Ratio	0.7	0.5	0.3	0.2	0.2
Embedding (%)	Pb–Pb	–	–	–	–	–
	Embedded	0.1–2.3	0.1–0.4	0.1–0.3	5.0	2.7
	Ratio	0.1–2.3	0.1–0.4	0.1–0.3	4.6	2.7
Tracking efficiency (%)	Pb–Pb	4.0	4.0	4.0	4.0	4.0
	Embedded	4.0	4.0	4.0	4.0	4.0
	Ratio	–	–	–	–	–
Tracking PYTHIA (%)	Pb–Pb	–	–	–	–	–
	Embedded	2.0	2.0	2.0	2.0	2.0
	Ratio	2.0	2.0	2.0	2.0	2.0
PYTHIA vs. pp (%)	Pb–Pb	–	–	–	–	–
	Embedded	5.0	5.0	5.0	2.0	2.0
	Ratio	5.0	5.0	5.0	2.0	2.0
Total (%)	Pb–Pb	4.0–4.1	4.1–4.3	4.3–4.5	8.0	9.0
	Embedded	6.8–7.2	6.8	6.8	9.8	8.7
	Ratio	5.5–5.9	5.4–5.5	5.4–5.6	8.8	10.3

Table 3
Table of systematic uncertainties for jet radial shapes for high-p_{T} associates (4–20 GeV/c) in Pb–Pb and embedded PYTHIA for the 0–10% most central collisions. Uncertainties are given as relative uncertainties in percentages. Note that relative uncertainties grow for higher r values.

Data sample	Pb–Pb			Embedded PYTHIA		
$p_{\mathrm{T,\,ch\,jet}}$ (GeV/c)	40–60	60–80	80–120	40–60	60–80	80–120
Background (%)	0.1–6.5	0.1–13.0	0.1–19.2	0.0–6.9	0.0–10.8	0.0–14.5
Mixed event corr. (%)	<0.1	<0.1	<0.1	<0.1	<0.1	<0.1
Embedding (%)	–	–	–	1.0–13.9	0.4–3.1	0.1–0.8
PYTHIA vs. pp (%)	–	–	–	2.0	2.0	2.0
Total (%)	0.1–6.5	0.1–13.0	0.1–19.2	2.2–15.7	2.0–11.5	2.0–14.6

Table 4
Table of systematic uncertainties for jet radial shapes for low-p_{T} associates (1–2 GeV/c, 2–3 GeV/c) in Pb–Pb and embedded PYTHIA for jets with $p_{\mathrm{T,\,ch\,jet}}$ = 40–60 GeV/c and for the 0–10% most central collisions. Uncertainties are given as relative uncertainties in percentages. Note that relative uncertainties grow for higher r values.

Data sample	Pb–Pb		Embedded PYTHIA	
$p_{\mathrm{T,\,assoc}}$ (GeV/c)	1–2	2–3	1–2	2–3
Background (%)	1.6–7.5	0.4–8.8	2.2–11.9	1.0–4.2
Mixed event corr. (%)	<0.1	<0.1	<0.1	<0.1
Embedding (%)	–	–	1.2–7.4	0.8–11.3
PYTHIA vs. pp (%)	–	–	2.0–10.0	2.0–10.0
Total (%)	1.6–7.5	0.4–8.8	6.2–13.0	4.5–15.7

description of the ITS-TPC matching efficiency. Another uncertainty from the tracking efficiency correction enters this analysis due to the usage of PYTHIA simulations. The tracking efficiency of the PYTHIA data is artificially lowered by 2% before embedding to account for the lower tracking efficiency in Pb–Pb collisions. As a conservative estimate, a relative uncertainty of 100% is assigned to this value. Both components of the tracking efficiency uncertainty are taken into account as independent contributions to the uncertainty, i.e. added in quadrature to the full uncertainty. These uncertainties are directly used as uncertainties for the yields, see Table 2. For the jet-associated yield ratio, the uncertainty on the tracking efficiency in Pb–Pb cancels, because it is correlated in Pb–Pb and the embedded PYTHIA reference. For the radial shape distribution, a change in the tracking efficiency has no impact either, since these observables are relative quantities that do not depend on the global magnitude of the tracking efficiency. As an alternative approach to estimate the impact of these two uncertainties of the tracking efficiencies on the observables, the full analysis was redone using corrections that assume the above given lower tracking efficiencies. There was no significant impact on the presented results.

Finally, an uncertainty is assigned since PYTHIA is used as a baseline instead of a measured pp reference. Including this uncertainty, the conclusions are also valid for a pp reference and not only for an embedded PYTHIA reference. In order to do so, the presented observables were calculated and compared for PYTHIA events and pp collisions at 7 TeV. Within the statistical precision of this comparison, it is only possible to give an estimate for the inclusive $p_{\mathrm{T,\,ch\,jet}}$-range. The relative deviations of each observable between both datasets enter directly as a systematic uncertainty and are on the level of a few percent, cf. Tables 2–4.

8. Results

Figs. 2 and 3 depict the jet-associated yields (left) and yield ratios (right) for high-p_{T} and low-p_{T} associated particles, respec-

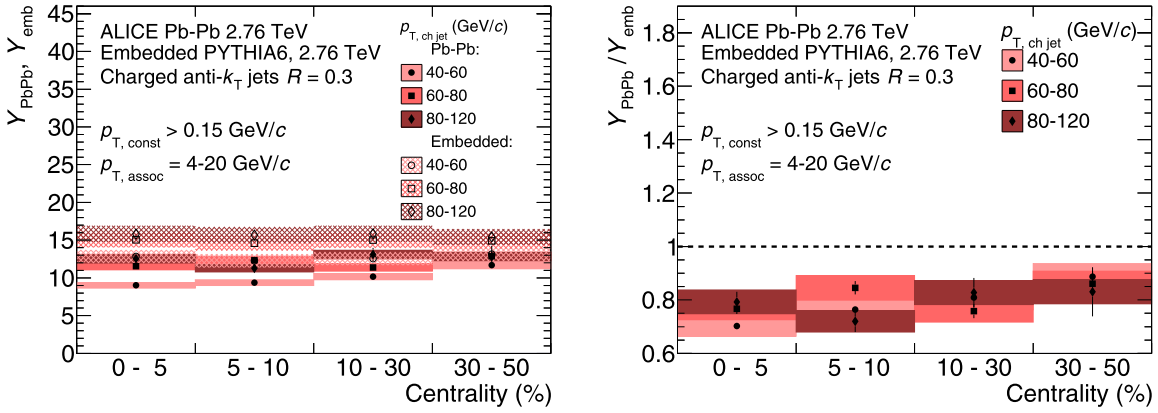

Fig. 2. Centrality dependence of jet-associated yields (left) and yield ratios (right) for high-p_T associates. Boxes represent systematic uncertainties, error bars represent statistical uncertainties. Observables are corrected for acceptance and background effects.

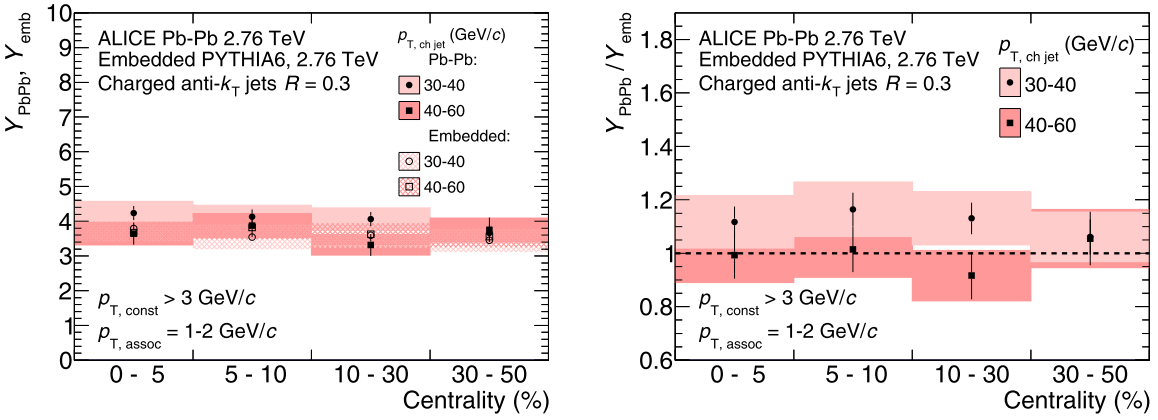

Fig. 3. Centrality dependence of jet-associated yields (left) and yield ratios (right) for low-p_T associates. Boxes represent systematic uncertainties, error bars represent statistical uncertainties. Observables are corrected for acceptance and background effects.

tively. Both quantities are shown as a function of event centrality and for several selected jet transverse momenta.

The jet-associated yield ratio shows a suppression with a significance of several standard deviations in the centrality range 0–50% for the considered high-p_T associated particles. In the probed jet momentum range, no significant $p_{T, ch jet}$-dependence is observed. The centrality-dependent linear slope of the distribution for $p_{T, ch jet} = 40$–60 GeV/c is more than one standard deviation away from zero, taking into account statistical and systematic uncertainties added in quadrature, indicating that there is a slightly stronger suppression for more central collisions in this case. As a cross check, the same observable was also measured for jets with several higher minimum $p_{T, const}$-cuts, i.e. 1, 2, and 3 GeV/c, which are less affected by the underlying event. They lead to similar conclusions.

The jet-associated yield ratio for low-p_T associates has much larger statistical and systematic uncertainties than the ratio of high-p_T constituents, thus it is not possible to draw a definite conclusion.

The measured jet relative radial shapes are presented in Figs. 4 and 5. The top panels show the self-normalized distributions, the difference and the ratio of the shapes in Pb–Pb and embedded PYTHIA can be found in the two lower panels. The jet radial shapes of high-p_T associates are measured for $p_{T, ch jet} = 40$–60 GeV/c, 60–80 GeV/c, and 80–120 GeV/c. Shapes of low-p_T associates are presented for jets with $p_{T, ch jet} = 30$–40 GeV/c and $p_{T, const} > 3$ GeV/c for associates with $p_{T, assoc} = 1$–2 GeV/c and $p_{T, assoc} = 2$–3 GeV/c.

In general, the radial shape measurements indicate that all jet-associated yields are similarly distributed relative to the jet axis in Pb–Pb and embedded PYTHIA. The yields of high-p_T associates appear to be slightly more collimated near the core for jets in Pb–Pb, though the absolute effect is small. While the shape is not significantly changed for jet transverse momenta between 40 and 60 GeV/c in Pb–Pb compared to the reference, there is a visible collimation for higher jet momenta above 60 GeV/c. This can be seen best in the difference distributions $\Delta_{PbPb-emb}$ of Fig. 4 which show that a larger fraction of the associated yield can be found near the core in Pb–Pb collisions.

The ratio distributions show that the collimation effect persists up to $r = 0.2$, which is best visible for jets with $p_{T, ch jet} = 60$–80 GeV/c. In the CMS measurement [50], no significant change of the near-side jet peak width is observed in Pb–Pb for high-p_T associates and jets above 120 GeV/c. However, the magnitude of the effect observed here is compatible with the observations within uncertainties. Also note that the CMS data hints as well to a small collimation of the peak for higher-p_T associates (4–8 GeV/c). Possible effects which might lead to a collimation include a relative change in the quark/gluon content in Pb–Pb compared to the reference [69], as well as a suppression of large-angle soft radiation in the coherent jet energy loss picture [70,71]. Low-p_T jet-associated yields presented in Fig. 5 are measured up to a distance of $r = 0.9$ relative to the jet since in this case the associates are decoupled from the trigger jets.

For $p_{T, assoc} = 1$–2 GeV/c, a hint of a broadening of the radial shape is observed for jets with momenta between 30 and 40 GeV/c

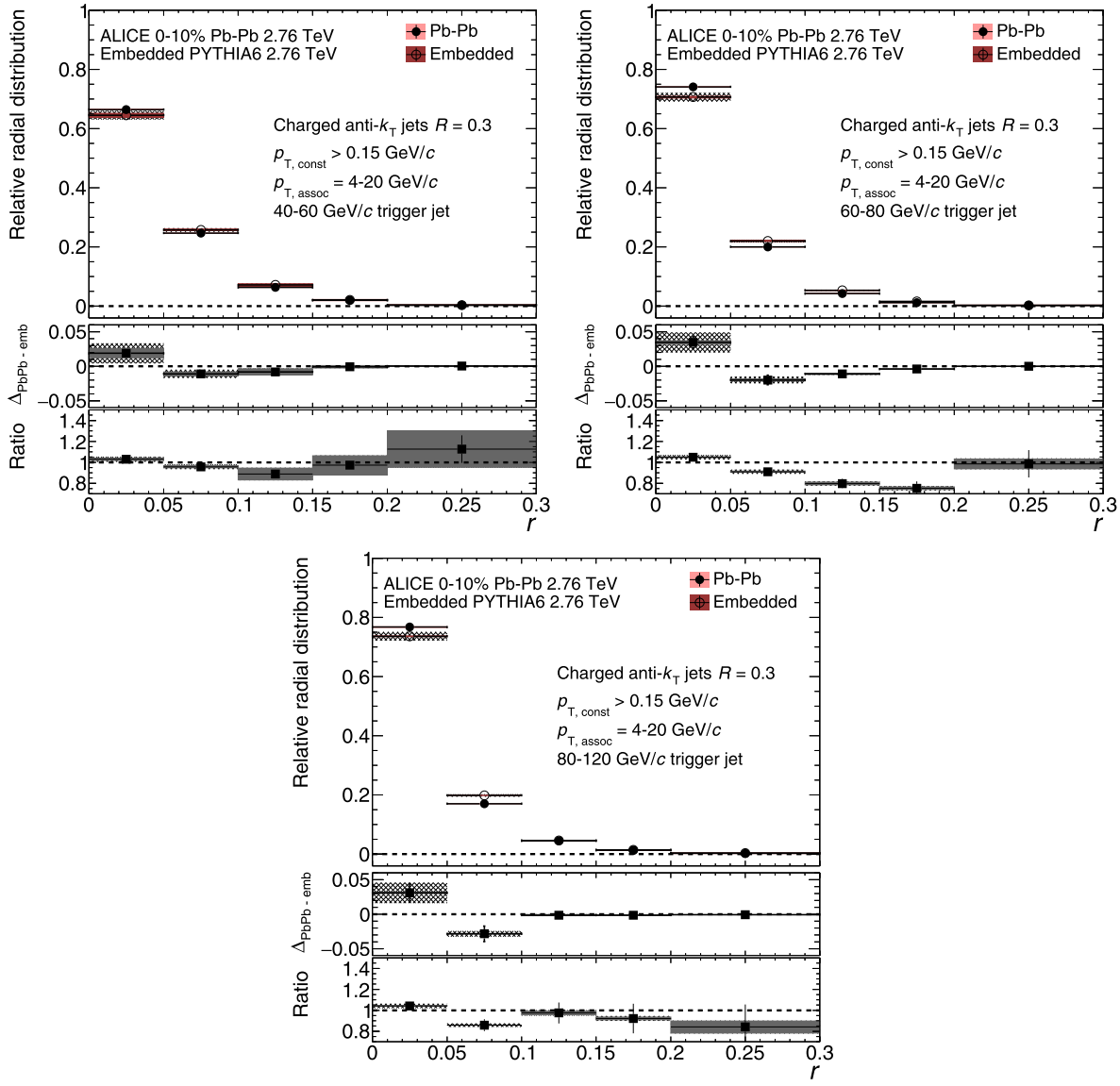

Fig. 4. Jet relative radial shape distributions, differences, and ratios for the 0–10% most central collisions for high-p_T constituents, shown for different jet transverse momenta. Boxes represent systematic uncertainties, shaded boxes include uncertainties from PYTHIA/pp comparison, and error bars represent statistical uncertainties. Observables are corrected for acceptance and background effects.

for the given definition. The broadening is visible in the difference distribution of the left plot in Fig. 5: in Pb–Pb collisions, a smaller fraction of particles can be found directly next to the jet axis. For higher associate transverse momenta, i.e. $p_{T,\text{assoc}} =$ 2–3 GeV/c, there is no significant modification of the low-p_T radial shape of jets in Pb–Pb collisions within the large current experimental uncertainties. A robust measurement of this observable for $p_{T,\text{ch jet}} =$ 40–60 GeV/c or higher momenta is not possible due to the insufficient size of the dataset. For higher jet momenta above 120 GeV/c, CMS measures a significant broadening of the near-side jet peak.

9. Summary

The presented results constitute the first attempt to study jet–hadron correlations with track-based jets down to transverse momenta of 30 GeV/c in Pb–Pb collisions — a challenging regime due to the large underlying event and its fluctuations. The jet radial shapes and the change in the particle p_T composition were measured in Pb–Pb collisions at $\sqrt{s_{NN}} = 2.76$ TeV for high- and low-p_T associates and compared to embedded PYTHIA simulations. The number of high-p_T associates in Pb–Pb collisions is suppressed compared to the reference by roughly 30 to 10%, depending on centrality. The radial particle distribution relative to the jet axis shows a moderate modification in Pb–Pb collisions with respect to PYTHIA. High-p_T associate particles are slightly more collimated in Pb–Pb collisions compared to the reference. For jets with $p_{T,\text{const}} \geq 3$ GeV/c, the radial distributions of low-p_T associates were measured. A hint of a broadening of the low-p_T radial shapes is observed for $p_{T,\text{assoc}} =$ 1–2 GeV/c. The shape for $p_{T,\text{assoc}} =$ 2–3 GeV/c does not show a significant modification within its large uncertainties. The results are in line with both previous jet–hadron-related measurements from the CMS Collaboration and jet shape measurements from the ALICE Collaboration at higher p_T and add further support for the established picture of in-medium parton energy loss.

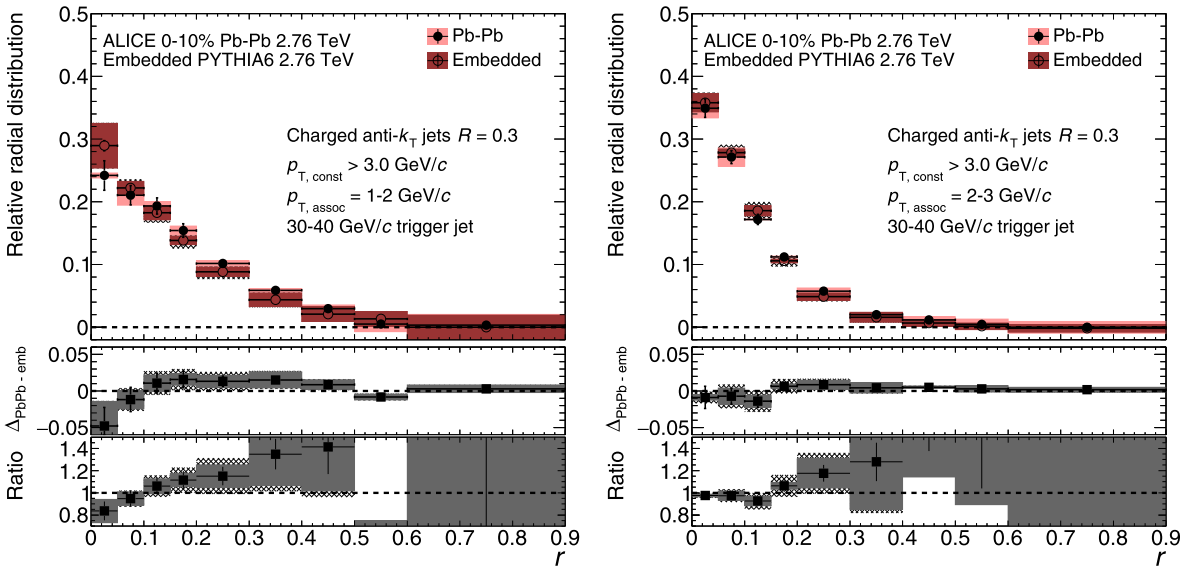

Fig. 5. Jet relative radial shape distributions, differences, and ratios for the 0–10% most central collisions for two different low-p_T constituent ranges. Boxes represent systematic uncertainties, shaded boxes include uncertainties from PYTHIA/pp comparison, and error bars represent statistical uncertainties. Observables are corrected for acceptance and background effects. The y-axis scale of the ratio is chosen to focus on $r < 0.3$, where the deviation of the ratio from unity is significant.

Acknowledgements

The ALICE Collaboration would like to thank all its engineers and technicians for their invaluable contributions to the construction of the experiment and the CERN accelerator teams for the outstanding performance of the LHC complex. The ALICE Collaboration gratefully acknowledges the resources and support provided by all Grid centers and the Worldwide LHC Computing Grid (WLCG) collaboration. The ALICE Collaboration acknowledges the following funding agencies for their support in building and running the ALICE detector: A.I. Alikhanyan National Science Laboratory (Yerevan Physics Institute) Foundation (ANSL), State Committee of Science and World Federation of Scientists (WFS), Armenia; Austrian Academy of Sciences, Austrian Science Fund (FWF): [M 2467-N36] and Nationalstiftung für Forschung, Technologie und Entwicklung, Austria; Ministry of Communications and High Technologies, National Nuclear Research Center, Azerbaijan; Conselho Nacional de Desenvolvimento Científico e Tecnológico (CNPq), Universidade Federal do Rio Grande do Sul (UFRGS), Financiadora de Estudos e Projetos (Finep) and Fundação de Amparo à Pesquisa do Estado de São Paulo (FAPESP), Brazil; Ministry of Science & Technology of China (MSTC), National Natural Science Foundation of China (NSFC) and Ministry of Education of China (MOEC), China; Croatian Science Foundation and Ministry of Science and Education, Croatia; Centro de Aplicaciones Tecnológicas y Desarrollo Nuclear (CEADEN), Cubaenergía, Cuba; Ministry of Education, Youth and Sports of the Czech Republic, Czech Republic; The Danish Council for Independent Research | Natural Sciences, the Carlsberg Foundation and Danish National Research Foundation (DNRF), Denmark; Helsinki Institute of Physics (HIP), Finland; Commissariat à l'Energie Atomique (CEA), Institut National de Physique Nucléaire et de Physique des Particules (IN2P3) and Centre National de la Recherche Scientifique (CNRS) and Région des Pays de la Loire, France; Bundesministerium für Bildung, Wissenschaft, Forschung und Technologie (BMBF) and GSI Helmholtzzentrum für Schwerionenforschung GmbH, Germany; General Secretariat for Research and Technology, Ministry of Education, Research and Religions, Greece; National Research, Development and Innovation Office, Hungary; Department of Atomic Energy, Government of India (DAE), Department of Science and Technology, Government of India (DST), University Grants Commission, Government of India (UGC) and Council of Scientific and Industrial Research (CSIR), India; Indonesian Institute of Science, Indonesia; Centro Fermi – Museo Storico della Fisica e Centro Studi e Ricerche Enrico Fermi and Istituto Nazionale di Fisica Nucleare (INFN), Italy; Institute for Innovative Science and Technology, Nagasaki Institute of Applied Science (IIST), Japan Society for the Promotion of Science (JSPS) KAKENHI and Japanese Ministry of Education, Culture, Sports, Science and Technology (MEXT), Japan; Consejo Nacional de Ciencia y Tecnología (CONACYT), through Fondo de Cooperación Internacional en Ciencia y Tecnología (FONCICYT) and Dirección General de Asuntos del Personal Academico (DGAPA), Mexico; Nederlandse Organisatie voor Wetenschappelijk Onderzoek (NWO), Netherlands; The Research Council of Norway, Norway; Commission on Science and Technology for Sustainable Development in the South (COMSATS), Pakistan; Pontificia Universidad Católica del Perú, Peru; Ministry of Science and Higher Education and National Science Centre, Poland; Korea Institute of Science and Technology Information and National Research Foundation of Korea (NRF), Republic of Korea; Ministry of Education and Scientific Research, Institute of Atomic Physics and Ministry of Research and Innovation and Institute of Atomic Physics, Romania; Joint Institute for Nuclear Research (JINR), Ministry of Education and Science of the Russian Federation, National Research Centre Kurchatov Institute, Russian Science Foundation and Russian Foundation for Basic Research, Russia; Ministry of Education, Science, Research and Sport of the Slovak Republic, Slovakia; National Research Foundation of South Africa, South Africa; Swedish Research Council (VR) and Knut & Alice Wallenberg Foundation (KAW), Sweden; European Organization for Nuclear Research, Switzerland; National Science and Technology Development Agency (NSDTA), Suranaree University of Technology (SUT) and Office of the Higher Education Commission under NRU project of Thailand, Thailand; Turkish Atomic Energy Authority (TAEK), Turkey; National Academy of Sciences of Ukraine, Ukraine; Science and Technology Facilities Council (STFC), United Kingdom; National Science Foundation of the United States of America (NSF) and U.S. Department of Energy, Office of Nuclear Physics (DOE NP), United States of America.

References

[1] HotQCD Collaboration, T. Bhattacharya, M.I. Buchoff, N.H. Christ, et al., QCD phase transition with chiral quarks and physical quark masses, Phys. Rev. Lett. 113 (2014) 082001, arXiv:1402.5175 [hep-lat].

[2] BRAHMS Collaboration, I. Arsene, et al., Quark–gluon plasma and color glass condensate at RHIC? The perspective from the BRAHMS experiment, Nucl. Phys. A 757 (1–2) (2005) 1–27, arXiv:nucl-ex/0410020.

[3] PHOBOS Collaboration, B. Back, et al., The PHOBOS perspective on discoveries at RHIC, Nucl. Phys. A 757 (1–2) (2005) 28–101, arXiv:nucl-ex/0410003.

[4] PHENIX Collaboration, K. Adcox, et al., Formation of dense partonic matter in relativistic nucleus–nucleus collisions at RHIC: experimental evaluation by the PHENIX collaboration, Nucl. Phys. A 757 (1–2) (2005) 184–283, arXiv:nucl-ex/0410022.

[5] STAR Collaboration, J. Adams, et al., Experimental and theoretical challenges in the search for the quark–gluon plasma: the STAR Collaboration's critical assessment of the evidence from RHIC collisions, Nucl. Phys. A 757 (1–2) (2005) 102–183, arXiv:nucl-ex/0501009.

[6] ALICE Collaboration, K. Aamodt, et al., Charged-particle multiplicity density at mid-rapidity in central Pb–Pb collisions at $\sqrt{s_{\rm NN}} = 2.76$ TeV, Phys. Rev. Lett. 105 (2010) 252301, arXiv:1011.3916 [nucl-ex].

[7] ALICE Collaboration, K. Aamodt, et al., Centrality dependence of the charged-particle multiplicity density at mid-rapidity in Pb–Pb collisions at $\sqrt{s_{\rm NN}} = 2.76$ TeV, Phys. Rev. Lett. 106 (2011) 032301, arXiv:1012.1657 [nucl-ex].

[8] CMS Collaboration, S. Chatrchyan, et al., Dependence on pseudorapidity and centrality of charged hadron production in Pb–Pb collisions at a nucleon-nucleon centre-of-mass energy of 2.76 TeV, J. High Energy Phys. 1108 (2011) 141, arXiv:1107.4800 [nucl-ex].

[9] ALICE Collaboration, K. Aamodt, et al., Two-pion Bose–Einstein correlations in central Pb–Pb collisions at $\sqrt{s_{\rm NN}} = 2.76$ TeV, Phys. Lett. B 696 (2011) 328–337, arXiv:1012.4035 [nucl-ex].

[10] ALICE Collaboration, K. Aamodt, et al., Elliptic flow of charged particles in Pb–Pb collisions at 2.76 TeV, Phys. Rev. Lett. 105 (2010) 252302, arXiv:1011.3914 [nucl-ex].

[11] ATLAS Collaboration, G. Aad, et al., Measurement of the pseudorapidity and transverse momentum dependence of the elliptic flow of charged particles in lead–lead collisions at $\sqrt{s_{\rm NN}} = 2.76$ TeV with the ATLAS detector, Phys. Lett. B 707 (2012) 330–348, arXiv:1108.6018 [hep-ex].

[12] CMS Collaboration, S. Chatrchyan, et al., Centrality dependence of dihadron correlations and azimuthal anisotropy harmonics in Pb–Pb collisions at $\sqrt{s_{\rm NN}} =$ 2.76 TeV, Eur. Phys. J. C 72 (2012) 2012, arXiv:1201.3158 [nucl-ex].

[13] ALICE Collaboration, K. Aamodt, et al., Higher harmonic anisotropic flow measurements of charged particles in Pb–Pb collisions at $\sqrt{s_{\rm NN}} = 2.76$ TeV, Phys. Rev. Lett. 107 (2011) 032301, arXiv:1105.3865 [nucl-ex].

[14] ATLAS Collaboration, G. Aad, et al., Measurement of the distributions of event-by-event flow harmonics in lead–lead collisions at 2.76 TeV with the ATLAS detector at the LHC, J. High Energy Phys. 1311 (2013) 183, arXiv:1305.2942 [hep-ex].

[15] CMS Collaboration, S. Chatrchyan, et al., Measurement of higher-order harmonic azimuthal anisotropy in Pb–Pb collisions at $\sqrt{s_{\rm NN}} = 2.76$ TeV, Phys. Rev. C 89 (2014) 044906, arXiv:1310.8651 [nucl-ex].

[16] ALICE Collaboration, K. Aamodt, et al., Suppression of charged particle production at large transverse momentum in central Pb–Pb collisions at $\sqrt{s_{\rm NN}} = 2.76$ TeV, Phys. Lett. B 696 (2011) 30–39, arXiv:1012.1004 [nucl-ex].

[17] CMS Collaboration, S. Chatrchyan, et al., Observation and studies of jet quenching in Pb–Pb collisions at nucleon-nucleon center-of-mass energy of 2.76 TeV, Phys. Rev. C 84 (2011) 024906, arXiv:1102.1957 [nucl-ex].

[18] M. Gyulassy, M. Plumer, Jet quenching in dense matter, Phys. Lett. B 243 (1990) 432–438.

[19] R. Baier, Y.L. Dokshitzer, S. Peigne, D. Schiff, Induced gluon radiation in a QCD medium, Phys. Lett. B 345 (1995) 277–286, arXiv:hep-ph/9411409 [hep-ph].

[20] C.A. Salgado, U.A. Wiedemann, Medium modification of jet shapes and jet multiplicities, Phys. Rev. Lett. 93 (2004) 042301, arXiv:hep-ph/0310079 [hep-ph].

[21] PHENIX Collaboration, K. Adcox, et al., Suppression of hadrons with large transverse momentum in central Au+Au collisions at $\sqrt{s_{\rm NN}} = 130$ GeV, Phys. Rev. Lett. 88 (2002) 022301, arXiv:nucl-ex/0109003 [nucl-ex].

[22] STAR Collaboration, C. Adler, et al., Disappearance of back-to-back high $p_{\rm T}$ hadron correlations in central Au+Au collisions at $\sqrt{s_{\rm NN}} = 200$ GeV, Phys. Rev. Lett. 90 (2003) 082302, arXiv:nucl-ex/0210033 [nucl-ex].

[23] STAR Collaboration, C. Adler, et al., Centrality dependence of high p_T hadron suppression in Au+Au collisions at $\sqrt{s_{\rm NN}} = 130$ GeV, Phys. Rev. Lett. 89 (2002) 202301, arXiv:nucl-ex/0206011 [nucl-ex].

[24] PHENIX Collaboration, K. Adcox, et al., Centrality dependence of the high-$p_{\rm T}$ charged hadron suppression in Au+Au collisions at $\sqrt{s_{\rm NN}} = 130$ GeV, Phys. Lett. B 561 (2003) 82–92, arXiv:nucl-ex/0207009 [nucl-ex].

[25] PHENIX Collaboration, S.S. Adler, et al., Suppressed π^0 production at large transverse momentum in central Au+Au collisions at $\sqrt{s_{\rm NN}} = 200$ GeV, Phys. Rev. Lett. 91 (2003) 072301, arXiv:nucl-ex/0304022.

[26] STAR Collaboration, J. Adams, et al., Transverse-momentum and collision-energy dependence of high-$p_{\rm T}$ hadron suppression in Au+Au collisions at ultrarelativistic energies, Phys. Rev. Lett. 91 (2003) 172302, arXiv:nucl-ex/0305015 [nucl-ex].

[27] STAR Collaboration, J. Adams, et al., Evidence from d+Au measurements for final state suppression of high-$p_{\rm T}$ hadrons in Au+Au collisions at RHIC, Phys. Rev. Lett. 91 (2003) 072304, arXiv:nucl-ex/0306024 [nucl-ex].

[28] PHOBOS Collaboration, B. Back, et al., Charged hadron transverse momentum distributions in Au+Au collisions at $\sqrt{s_{\rm NN}} = 200$ GeV, Phys. Lett. B 578 (2004) 297–303, arXiv:nucl-ex/0302015 [nucl-ex].

[29] BRAHMS Collaboration, I. Arsene, et al., Transverse momentum spectra in Au+Au and d+Au collisions at $\sqrt{s_{\rm NN}} = 200$ GeV and the pseudorapidity dependence of high-$p_{\rm T}$suppression, Phys. Rev. Lett. 91 (2003) 072305, arXiv:nucl-ex/0307003 [nucl-ex].

[30] STAR Collaboration, J. Adams, et al., Direct observation of dijets in central Au–Au collisions at $\sqrt{s_{\rm NN}} = 200$ GeV, Phys. Rev. Lett. 97 (2006) 162301, arXiv:nucl-ex/0604018 [nucl-ex].

[31] PHENIX Collaboration, A. Adare, et al., System size and energy dependence of jet-induced hadron pair correlation shapes in Cu+Cu and Au+Au collisions at $\sqrt{s_{\rm NN}} = 200$ and 62.4 GeV, Phys. Rev. Lett. 98 (2007) 232302, arXiv:nucl-ex/0611019 [nucl-ex].

[32] PHENIX Collaboration, A. Adare, et al., Quantitative constraints on the opacity of hot partonic matter from semi-inclusive single high transverse momentum pion suppression in Au+Au collisions at $\sqrt{s_{\rm NN}} = 200$ GeV, Phys. Rev. C 77 (2008) 064907, arXiv:0801.1665 [nucl-ex].

[33] STAR Collaboration, L. Adamczyk, et al., Jet-hadron correlations in $\sqrt{s_{NN}} = 200$ GeV $p + p$ and central Au+Au collisions, Phys. Rev. Lett. 112 (12) (2014) 122301, arXiv:1302.6184 [nucl-ex].

[34] STAR Collaboration, L. Adamczyk, et al., Measurements of jet quenching with semi-inclusive hadron-jet distributions in Au–Au collisions at $\sqrt{s_{\rm NN}} = 200$ GeV, Phys. Rev. C 96 (2) (2017) 024905, arXiv:1702.01108 [nucl-ex].

[35] ATLAS Collaboration, G. Aad, et al., Observation of a centrality-dependent dijet asymmetry in Pb–Pb collisions at $\sqrt{s_{\rm NN}} = 2.76$ TeV with the ATLAS Detector at the LHC, Phys. Rev. Lett. 105 (2010) 252303, arXiv:1011.6182 [hep-ex].

[36] ALICE Collaboration, K. Aamodt, et al., Particle-yield modification in jet-like azimuthal di-hadron correlations in Pb–Pb collisions at $\sqrt{s_{\rm NN}} = 2.76$ TeV, Phys. Rev. Lett. 108 (2012) 092301, arXiv:1110.0121 [nucl-ex].

[37] CMS Collaboration, S. Chatrchyan, et al., Study of high-$p_{\rm T}$charged particle suppression in Pb–Pb compared to pp collisions at $\sqrt{s_{\rm NN}} = 2.76$ TeV, Eur. Phys. J. C 72 (2012) 1945, arXiv:1202.2554 [nucl-ex].

[38] CMS Collaboration, S. Chatrchyan, et al., Jet momentum dependence of jet quenching in Pb–Pb collisions at $\sqrt{s_{\rm NN}} = 2.76$ TeV, Phys. Lett. B 712 (2012) 176–197, arXiv:1202.5022 [nucl-ex].

[39] CMS Collaboration, S. Chatrchyan, et al., Measurement of jet fragmentation into charged particles in pp and Pb–Pb collisions at $\sqrt{s_{\rm NN}} = 2.76$ TeV, J. High Energy Phys. 1210 (2012) 087, arXiv:1205.5872 [nucl-ex].

[40] CMS Collaboration, S. Chatrchyan, et al., Studies of jet quenching using isolated-photon+jet correlations in Pb–Pb and pp collisions at $\sqrt{s_{\rm NN}} = 2.76$ TeV, Phys. Lett. B 718 (2013) 773–794, arXiv:1205.0206 [nucl-ex].

[41] ATLAS Collaboration, G. Aad, et al., Measurement of the jet radius and transverse momentum dependence of inclusive jet suppression in lead–lead collisions at $\sqrt{s_{\rm NN}} = 2.76$ TeV with the ATLAS detector, Phys. Lett. B 719 (2013) 220–241, arXiv:1208.1967 [hep-ex].

[42] CMS Collaboration, S. Chatrchyan, et al., Evidence of b-jet quenching in Pb–Pb collisions at $\sqrt{s_{\rm NN}} = 2.76$ TeV, Phys. Rev. Lett. 113 (13) (2014) 132301, arXiv:1312.4198 [nucl-ex].

[43] CMS Collaboration, S. Chatrchyan, et al., Modification of jet shapes in Pb–Pb collisions at $\sqrt{s_{\rm NN}} = 2.76$ TeV, Phys. Lett. B 730 (2014) 243–263, arXiv:1310.0878 [nucl-ex].

[44] CMS Collaboration, S. Chatrchyan, et al., Measurement of jet fragmentation in Pb–Pb and pp collisions at $\sqrt{s_{\rm NN}} = 2.76$ TeV, Phys. Rev. C 90 (2) (2014) 024908, arXiv:1406.0932 [nucl-ex].

[45] ATLAS Collaboration, G. Aad, et al., Measurement of inclusive jet charged-particle fragmentation functions in Pb–Pb collisions at $\sqrt{s_{\rm NN}} = 2.76$ TeV with the ATLAS detector, Phys. Lett. B 739 (2014) 320–342, arXiv:1406.2979 [hep-ex].

[46] ATLAS Collaboration, G. Aad, et al., Measurements of the nuclear modification factor for jets in Pb–Pb collisions at $\sqrt{s_{\rm NN}} = 2.76$ TeV with the ATLAS detector, Phys. Rev. Lett. 114 (7) (2015) 072302, arXiv:1411.2357 [hep-ex].

[47] ALICE Collaboration, J. Adam, et al., Measurement of jet quenching with semi-inclusive hadron-jet distributions in central Pb–Pb collisions at $\sqrt{s_{\rm NN}} = 2.76$ TeV, J. High Energy Phys. 09 (2015) 170, arXiv:1506.03984 [nucl-ex].

[48] ALICE Collaboration, J. Adam, et al., Anomalous evolution of the near-side jet peak shape in Pb–Pb collisions at $\sqrt{s_{\rm NN}} = 2.76$ TeV, Phys. Rev. Lett. 119 (2017) 102301, arXiv:1609.06643 [nucl-ex].

[49] ALICE Collaboration, J. Adam, et al., Evolution of the longitudinal and azimuthal structure of the near-side jet peak in Pb–Pb collisions at $\sqrt{s_{\rm NN}} = 2.76$ TeV, Phys. Rev. C 96 (2017) 034904, arXiv:1609.06667 [nucl-ex].

[50] CMS Collaboration, Correlations between jets and charged particles in PbPb and pp collisions at $\sqrt{s_{\rm NN}} = 2.76$ TeV, J. High Energy Phys. 1602 (2016) 156, arXiv:1601.00079 [nucl-ex].
[51] ALICE Collaboration, S. Acharya, et al., Medium modification of the shape of small-radius jets in central Pb–Pb collisions at $\sqrt{s_{\rm NN}} = 2.76$ TeV, J. High Energy Phys. 10 (2018) 139, arXiv:1807.06854 [nucl-ex].
[52] T. Sjostrand, S. Mrenna, P.Z. Skands, PYTHIA 6.4 physics and manual, J. High Energy Phys. 0605 (2006) 026, arXiv:hep-ph/0603175 [hep-ph].
[53] ALICE Collaboration, K. Aamodt, et al., The ALICE experiment at the CERN LHC, J. Instrum. 3 (2008) S08002.
[54] ALICE Collaboration, B.B. Abelev, et al., Performance of the ALICE experiment at the CERN LHC, Int. J. Mod. Phys. A 29 (2014) 1430044, arXiv:1402.4476 [nucl-ex].
[55] ALICE Collaboration, B. Abelev, et al., Centrality determination of Pb–Pb collisions at $\sqrt{s_{\rm NN}} = 2.76$ TeV with ALICE, Phys. Rev. C 88 (4) (2013) 044909, arXiv:1301.4361 [nucl-ex].
[56] ALICE Collaboration, B. Abelev, et al., Centrality dependence of charged particle production at large transverse momentum in Pb–Pb collisions at $\sqrt{s_{\rm NN}} = 2.76$ TeV, Phys. Lett. B 720 (2013) 52–62, arXiv:1208.2711 [hep-ex].
[57] X.-N. Wang, M. Gyulassy, HIJING: a Monte Carlo model for multiple jet production in pp, pA and AA collisions, Phys. Rev. D 44 (1991) 3501.
[58] R. Brun, F. Carminati, S. Giani, GEANT Detector Description and Simulation Tool, CERN Program Library Long Write-up, W5013, 1994.
[59] ALICE Collaboration, The ALICE definition of primary particles, ALICE-PUBLIC-2017-005, https://cds.cern.ch/record/2270008, 2017.
[60] ALICE Collaboration, B. Abelev, et al., Long-range angular correlations of π, K and p in p–Pb collisions at $\sqrt{s_{\rm NN}} = 5.02$ TeV, Phys. Lett. B 726 (2013) 164–177, arXiv:1307.3237 [nucl-ex].
[61] ALICE Collaboration, J. Adam, et al., Pseudorapidity dependence of the anisotropic flow of charged particles in Pb–Pb collisions at $\sqrt{s_{\rm NN}} = 2.76$ TeV, Phys. Lett. B 762 (2016) 376–388, arXiv:1605.02035 [nucl-ex].
[62] M. Cacciari, J. Rojo, G.P. Salam, G. Soyez, Jet reconstruction in heavy ion collisions, Eur. Phys. J. C 71 (2011) 1539, arXiv:1010.1759 [hep-ph].
[63] M. Cacciari, G.P. Salam, G. Soyez, The Anti-k(t) jet clustering algorithm, J. High Energy Phys. 0804 (2008) 063, arXiv:0802.1189 [hep-ph].
[64] M. Cacciari, G.P. Salam, G. Soyez, FastJet user manual, Eur. Phys. J. C 72 (2012) 1896, arXiv:1111.6097 [hep-ph].
[65] ALICE Collaboration, B. Abelev, et al., Measurement of event background fluctuations for charged particle jet reconstruction in Pb–Pb collisions at $\sqrt{s_{\rm NN}} = 2.76$ TeV, J. High Energy Phys. 1203 (2012) 053, arXiv:1201.2423 [hep-ex].
[66] ALICE Collaboration, B. Abelev, et al., Measurement of charged jet suppression in Pb–Pb collisions at $\sqrt{s_{\rm NN}} = 2.76$ TeV, J. High Energy Phys. 1403 (2014) 013, arXiv:1311.0633 [nucl-ex].
[67] ALICE Collaboration, Supplemental figures for measurement of jet radial profiles in Pb–Pb collisions at $\sqrt{s_{NN}} = 2.76$ TeV, ALICE-PUBLIC-2019-002, https://cds.cern.ch/record/2672661, 2019.
[68] P.Z. Skands, Tuning Monte Carlo generators: the Perugia tunes, Phys. Rev. D 82 (2010) 074018, arXiv:1005.3457 [hep-ph].
[69] M. Spousta, B. Cole, Interpreting single jet measurements in Pb+Pb collisions at the LHC, Eur. Phys. J. C 76 (2) (2016) 50, arXiv:1504.05169 [hep-ph].
[70] J. Casalderrey-Solana, J.G. Milhano, U.A. Wiedemann, Jet quenching via jet collimation, J. Phys. G 38 (2011) 035006, arXiv:1012.0745 [hep-ph].
[71] J. Casalderrey-Solana, Y. Mehtar-Tani, C.A. Salgado, K. Tywoniuk, New picture of jet quenching dictated by color coherence, Phys. Lett. B 725 (2013) 357–360, arXiv:1210.7765 [hep-ph].

ALICE Collaboration

S. Acharya [141], D. Adamová [93], S.P. Adhya [141], A. Adler [74], J. Adolfsson [80], M.M. Aggarwal [98], G. Aglieri Rinella [34], M. Agnello [31], N. Agrawal [10], Z. Ahammed [141], S. Ahmad [17], S.U. Ahn [76], S. Aiola [146], A. Akindinov [64], M. Al-Turany [105], S.N. Alam [141], D.S.D. Albuquerque [122], D. Aleksandrov [87], B. Alessandro [58], H.M. Alfanda [6], R. Alfaro Molina [72], B. Ali [17], Y. Ali [15], A. Alici [10,53,27], A. Alkin [2], J. Alme [22], T. Alt [69], L. Altenkamper [22], I. Altsybeev [112], M.N. Anaam [6], C. Andrei [47], D. Andreou [34], H.A. Andrews [109], A. Andronic [144], M. Angeletti [34], V. Anguelov [102], C. Anson [16], T. Antičić [106], F. Antinori [56], P. Antonioli [53], R. Anwar [126], N. Apadula [79], L. Aphecetche [114], H. Appelshäuser [69], S. Arcelli [27], R. Arnaldi [58], M. Arratia [79], I.C. Arsene [21], M. Arslandok [102], A. Augustinus [34], R. Averbeck [105], S. Aziz [61], M.D. Azmi [17], A. Badalà [55], Y.W. Baek [40], S. Bagnasco [58], X. Bai [105], R. Bailhache [69], R. Bala [99], A. Baldisseri [137], M. Ball [42], R.C. Baral [85], R. Barbera [28], L. Barioglio [26], G.G. Barnaföldi [145], L.S. Barnby [92], V. Barret [134], P. Bartalini [6], K. Barth [34], E. Bartsch [69], F. Baruffaldi [29], N. Bastid [134], S. Basu [143], G. Batigne [114], B. Batyunya [75], P.C. Batzing [21], D. Bauri [48], J.L. Bazo Alba [110], I.G. Bearden [88], C. Bedda [63], N.K. Behera [60], I. Belikov [136], F. Bellini [34], R. Bellwied [126], V. Belyaev [91], G. Bencedi [145], S. Beole [26], A. Bercuci [47], Y. Berdnikov [96], D. Berenyi [145], R.A. Bertens [130], D. Berzano [58], M.G. Besoiu [68], L. Betev [34], A. Bhasin [99], I.R. Bhat [99], H. Bhatt [48], B. Bhattacharjee [41], A. Bianchi [26], L. Bianchi [126,26], N. Bianchi [51], J. Bielčík [37], J. Bielčíková [93], A. Bilandzic [117,103], G. Biro [145], R. Biswas [3], S. Biswas [3], J.T. Blair [119], D. Blau [87], C. Blume [69], G. Boca [139], F. Bock [94,34], A. Bogdanov [91], L. Boldizsár [145], A. Bolozdynya [91], M. Bombara [38], G. Bonomi [140], H. Borel [137], A. Borissov [144,91], M. Borri [128], H. Bossi [146], E. Botta [26], C. Bourjau [88], L. Bratrud [69], P. Braun-Munzinger [105], M. Bregant [121], T.A. Broker [69], M. Broz [37], E.J. Brucken [43], E. Bruna [58], G.E. Bruno [33,104], M.D. Buckland [128], D. Budnikov [107], H. Buesching [69], S. Bufalino [31], O. Bugnon [114], P. Buhler [113], P. Buncic [34], Z. Buthelezi [73], J.B. Butt [15], J.T. Buxton [95], D. Caffarri [89], A. Caliva [105], E. Calvo Villar [110], R.S. Camacho [44], P. Camerini [25], A.A. Capon [113], F. Carnesecchi [10], J. Castillo Castellanos [137], A.J. Castro [130], E.A.R. Casula [54], F. Catalano [31], C. Ceballos Sanchez [52], P. Chakraborty [48], S. Chandra [141], B. Chang [127], W. Chang [6], S. Chapeland [34], M. Chartier [128], S. Chattopadhyay [141], S. Chattopadhyay [108], A. Chauvin [24], C. Cheshkov [135], B. Cheynis [135], V. Chibante Barroso [34], D.D. Chinellato [122], S. Cho [60], P. Chochula [34], T. Chowdhury [134], P. Christakoglou [89], C.H. Christensen [88], P. Christiansen [80], T. Chujo [133], C. Cicalo [54], L. Cifarelli [10,27], F. Cindolo [53], J. Cleymans [125], F. Colamaria [52], D. Colella [52], A. Collu [79], M. Colocci [27], M. Concas [58,ii], G. Conesa Balbastre [78], Z. Conesa del Valle [61], G. Contin [59,128], J.G. Contreras [37], T.M. Cormier [94], Y. Corrales Morales [58,26], P. Cortese [32], M.R. Cosentino [123], F. Costa [34], S. Costanza [139], J. Crkovská [61], P. Crochet [134], E. Cuautle [70], L. Cunqueiro [94], D. Dabrowski [142], T. Dahms [103,117], A. Dainese [56],

F.P.A. Damas [137,114], S. Dani [66], M.C. Danisch [102], A. Danu [68], D. Das [108], I. Das [108], S. Das [3], A. Dash [85], S. Dash [48], A. Dashi [103], S. De [85,49], A. De Caro [30], G. de Cataldo [52], C. de Conti [121], J. de Cuveland [39], A. De Falco [24], D. De Gruttola [10], N. De Marco [58], S. De Pasquale [30], R.D. De Souza [122], S. Deb [49], H.F. Degenhardt [121], K.R. Deja [142], A. Deloff [84], S. Delsanto [131,26], P. Dhankher [48], D. Di Bari [33], A. Di Mauro [34], R.A. Diaz [8], T. Dietel [125], P. Dillenseger [69], Y. Ding [6], R. Divià [34], Ø. Djuvsland [22], U. Dmitrieva [62], A. Dobrin [34,68], B. Dönigus [69], O. Dordic [21], A.K. Dubey [141], A. Dubla [105], S. Dudi [98], M. Dukhishyam [85], P. Dupieux [134], R.J. Ehlers [146], D. Elia [52], H. Engel [74], E. Epple [146], B. Erazmus [114], F. Erhardt [97], A. Erokhin [112], M.R. Ersdal [22], B. Espagnon [61], G. Eulisse [34], J. Eum [18], D. Evans [109], S. Evdokimov [90], L. Fabbietti [117,103], M. Faggin [29], J. Faivre [78], A. Fantoni [51], M. Fasel [94], P. Fecchio [31], L. Feldkamp [144], A. Feliciello [58], G. Feofilov [112], A. Fernández Téllez [44], A. Ferrero [137], A. Ferretti [26], A. Festanti [34], V.J.G. Feuillard [102], J. Figiel [118], S. Filchagin [107], D. Finogeev [62], F.M. Fionda [22], G. Fiorenza [52], F. Flor [126], S. Foertsch [73], P. Foka [105], S. Fokin [87], E. Fragiacomo [59], U. Frankenfeld [105], G.G. Fronze [26], U. Fuchs [34], C. Furget [78], A. Furs [62], M. Fusco Girard [30], J.J. Gaardhøje [88], M. Gagliardi [26], A.M. Gago [110], A. Gal [136], C.D. Galvan [120], P. Ganoti [83], C. Garabatos [105], E. Garcia-Solis [11], K. Garg [28], C. Gargiulo [34], K. Garner [144], P. Gasik [103,117], E.F. Gauger [119], M.B. Gay Ducati [71], M. Germain [114], J. Ghosh [108], P. Ghosh [141], S.K. Ghosh [3], P. Gianotti [51], P. Giubellino [105,58], P. Giubilato [29], P. Glässel [102], D.M. Goméz Coral [72], A. Gomez Ramirez [74], V. Gonzalez [105], P. González-Zamora [44], S. Gorbunov [39], L. Görlich [118], S. Gotovac [35], V. Grabski [72], L.K. Graczykowski [142], K.L. Graham [109], L. Greiner [79], A. Grelli [63], C. Grigoras [34], V. Grigoriev [91], A. Grigoryan [1], S. Grigoryan [75], O.S. Groettvik [22], J.M. Gronefeld [105], F. Grosa [31], J.F. Grosse-Oetringhaus [34], R. Grosso [105], R. Guernane [78], B. Guerzoni [27], M. Guittiere [114], K. Gulbrandsen [88], T. Gunji [132], A. Gupta [99], R. Gupta [99], I.B. Guzman [44], R. Haake [34,146], M.K. Habib [105], C. Hadjidakis [61], H. Hamagaki [81], G. Hamar [145], M. Hamid [6], R. Hannigan [119], M.R. Haque [63], A. Harlenderova [105], J.W. Harris [146], A. Harton [11], J.A. Hasenbichler [34], H. Hassan [78], D. Hatzifotiadou [10,53], P. Hauer [42], S. Hayashi [132], S.T. Heckel [69], E. Hellbär [69], H. Helstrup [36], A. Herghelegiu [47], E.G. Hernandez [44], G. Herrera Corral [9], F. Herrmann [144], K.F. Hetland [36], T.E. Hilden [43], H. Hillemanns [34], C. Hills [128], B. Hippolyte [136], B. Hohlweger [103], D. Horak [37], S. Hornung [105], R. Hosokawa [133], P. Hristov [34], C. Huang [61], C. Hughes [130], P. Huhn [69], T.J. Humanic [95], H. Hushnud [108], L.A. Husova [144], N. Hussain [41], S.A. Hussain [15], T. Hussain [17], D. Hutter [39], D.S. Hwang [19], J.P. Iddon [128,34], R. Ilkaev [107], M. Inaba [133], M. Ippolitov [87], M.S. Islam [108], M. Ivanov [105], V. Ivanov [96], V. Izucheev [90], B. Jacak [79], N. Jacazio [27], P.M. Jacobs [79], M.B. Jadhav [48], S. Jadlovska [116], J. Jadlovsky [116], S. Jaelani [63], C. Jahnke [121], M.J. Jakubowska [142], M.A. Janik [142], M. Jercic [97], O. Jevons [109], R.T. Jimenez Bustamante [105], M. Jin [126], F. Jonas [144,94], P.G. Jones [109], A. Jusko [109], P. Kalinak [65], A. Kalweit [34], J.H. Kang [147], V. Kaplin [91], S. Kar [6], A. Karasu Uysal [77], O. Karavichev [62], T. Karavicheva [62], P. Karczmarczyk [34], E. Karpechev [62], U. Kebschull [74], R. Keidel [46], M. Keil [34], B. Ketzer [42], Z. Khabanova [89], A.M. Khan [6], S. Khan [17], S.A. Khan [141], A. Khanzadeev [96], Y. Kharlov [90], A. Khatun [17], A. Khuntia [118,49], B. Kileng [36], B. Kim [60], B. Kim [133], D. Kim [147], D.J. Kim [127], E.J. Kim [13], H. Kim [147], J. Kim [147], J.S. Kim [40], J. Kim [102], J. Kim [147], J. Kim [13], M. Kim [102], S. Kim [19], T. Kim [147], T. Kim [147], S. Kirsch [39], I. Kisel [39], S. Kiselev [64], A. Kisiel [142], J.L. Klay [5], C. Klein [69], J. Klein [58], S. Klein [79], C. Klein-Bösing [144], S. Klewin [102], A. Kluge [34], M.L. Knichel [34], A.G. Knospe [126], C. Kobdaj [115], M.K. Köhler [102], T. Kollegger [105], A. Kondratyev [75], N. Kondratyeva [91], E. Kondratyuk [90], P.J. Konopka [34], L. Koska [116], O. Kovalenko [84], V. Kovalenko [112], M. Kowalski [118], I. Králik [65], A. Kravčáková [38], L. Kreis [105], M. Krivda [109,65], F. Krizek [93], K. Krizkova Gajdosova [37], M. Krüger [69], E. Kryshen [96], M. Krzewicki [39], A.M. Kubera [95], V. Kučera [60], C. Kuhn [136], P.G. Kuijer [89], L. Kumar [98], S. Kumar [48], S. Kundu [85], P. Kurashvili [84], A. Kurepin [62], A.B. Kurepin [62], S. Kushpil [93], J. Kvapil [109], M.J. Kweon [60], J.Y. Kwon [60], Y. Kwon [147], S.L. La Pointe [39], P. La Rocca [28], Y.S. Lai [79], R. Langoy [124], K. Lapidus [34,146], A. Lardeux [21], P. Larionov [51], E. Laudi [34], R. Lavicka [37], T. Lazareva [112], R. Lea [25], L. Leardini [102], S. Lee [147], F. Lehas [89], S. Lehner [113], J. Lehrbach [39], R.C. Lemmon [92], I. León Monzón [120], E.D. Lesser [20], M. Lettrich [34], P. Lévai [145], X. Li [12], X.L. Li [6], J. Lien [124], R. Lietava [109], B. Lim [18], S. Lindal [21], V. Lindenstruth [39], S.W. Lindsay [128], C. Lippmann [105], M.A. Lisa [95], V. Litichevskyi [43], A. Liu [79], S. Liu [95], W.J. Llope [143], I.M. Lofnes [22], V. Loginov [91], C. Loizides [94], P. Loncar [35], X. Lopez [134], E. López Torres [8], P. Luettig [69], J.R. Luhder [144], M. Lunardon [29], G. Luparello [59], M. Lupi [74], A. Maevskaya [62], M. Mager [34], S.M. Mahmood [21], T. Mahmoud [42], A. Maire [136], R.D. Majka [146], M. Malaev [96], Q.W. Malik [21], L. Malinina [75,iii], D. Mal'Kevich [64], P. Malzacher [105], A. Mamonov [107], V. Manko [87], F. Manso [134],

V. Manzari [52], Y. Mao [6], M. Marchisone [135], J. Mareš [67], G.V. Margagliotti [25], A. Margotti [53], J. Margutti [63], A. Marín [105], C. Markert [119], M. Marquard [69], N.A. Martin [102], P. Martinengo [34], J.L. Martinez [126], M.I. Martínez [44], G. Martínez García [114], M. Martinez Pedreira [34], S. Masciocchi [105], M. Masera [26], A. Masoni [54], L. Massacrier [61], E. Masson [114], A. Mastroserio [52,138], A.M. Mathis [103,117], P.F.T. Matuoka [121], A. Matyja [118], C. Mayer [118], M. Mazzilli [33], M.A. Mazzoni [57], A.F. Mechler [69], F. Meddi [23], Y. Melikyan [91], A. Menchaca-Rocha [72], E. Meninno [30], M. Meres [14], S. Mhlanga [125], Y. Miake [133], L. Micheletti [26], M.M. Mieskolainen [43], D.L. Mihaylov [103], K. Mikhaylov [64,75], A. Mischke [63,i], A.N. Mishra [70], D. Miśkowiec [105], C.M. Mitu [68], N. Mohammadi [34], A.P. Mohanty [63], B. Mohanty [85], M. Mohisin Khan [17,iv], M. Mondal [141], M.M. Mondal [66], C. Mordasini [103], D.A. Moreira De Godoy [144], L.A.P. Moreno [44], S. Moretto [29], A. Morreale [114], A. Morsch [34], T. Mrnjavac [34], V. Muccifora [51], E. Mudnic [35], D. Mühlheim [144], S. Muhuri [141], J.D. Mulligan [79,146], M.G. Munhoz [121], K. Münning [42], R.H. Munzer [69], H. Murakami [132], S. Murray [73], L. Musa [34], J. Musinsky [65], C.J. Myers [126], J.W. Myrcha [142], B. Naik [48], R. Nair [84], B.K. Nandi [48], R. Nania [10,53], E. Nappi [52], M.U. Naru [15], A.F. Nassirpour [80], H. Natal da Luz [121], C. Nattrass [130], R. Nayak [48], T.K. Nayak [85,141], S. Nazarenko [107], R.A. Negrao De Oliveira [69], L. Nellen [70], S.V. Nesbo [36], G. Neskovic [39], B.S. Nielsen [88], S. Nikolaev [87], S. Nikulin [87], V. Nikulin [96], F. Noferini [10,53], P. Nomokonov [75], G. Nooren [63], J. Norman [78], P. Nowakowski [142], A. Nyanin [87], J. Nystrand [22], M. Ogino [81], A. Ohlson [102], J. Oleniacz [142], A.C. Oliveira Da Silva [121], M.H. Oliver [146], C. Oppedisano [58], R. Orava [43], A. Ortiz Velasquez [70], A. Oskarsson [80], J. Otwinowski [118], K. Oyama [81], Y. Pachmayer [102], V. Pacik [88], D. Pagano [140], G. Paić [70], P. Palni [6], J. Pan [143], A.K. Pandey [48], S. Panebianco [137], V. Papikyan [1], P. Pareek [49], J. Park [60], J.E. Parkkila [127], S. Parmar [98], A. Passfeld [144], S.P. Pathak [126], R.N. Patra [141], B. Paul [24,58], H. Pei [6], T. Peitzmann [63], X. Peng [6], L.G. Pereira [71], H. Pereira Da Costa [137], D. Peresunko [87], G.M. Perez [8], E. Perez Lezama [69], V. Peskov [69], Y. Pestov [4], V. Petráček [37], M. Petrovici [47], R.P. Pezzi [71], S. Piano [59], M. Pikna [14], P. Pillot [114], L.O.D.L. Pimentel [88], O. Pinazza [53,34], L. Pinsky [126], S. Pisano [51], D.B. Piyarathna [126], M. Płoskoń [79], M. Planinic [97], F. Pliquett [69], J. Pluta [142], S. Pochybova [145], M.G. Poghosyan [94], B. Polichtchouk [90], N. Poljak [97], W. Poonsawat [115], A. Pop [47], H. Poppenborg [144], S. Porteboeuf-Houssais [134], V. Pozdniakov [75], S.K. Prasad [3], R. Preghenella [53], F. Prino [58], C.A. Pruneau [143], I. Pshenichnov [62], M. Puccio [34,26], V. Punin [107], K. Puranapanda [141], J. Putschke [143], R.E. Quishpe [126], S. Ragoni [109], S. Raha [3], S. Rajput [99], J. Rak [127], A. Rakotozafindrabe [137], L. Ramello [32], F. Rami [136], R. Raniwala [100], S. Raniwala [100], S.S. Räsänen [43], B.T. Rascanu [69], R. Rath [49], V. Ratza [42], I. Ravasenga [31], K.F. Read [130,94], K. Redlich [84,v], A. Rehman [22], P. Reichelt [69], F. Reidt [34], X. Ren [6], R. Renfordt [69], A. Reshetin [62], J.-P. Revol [10], K. Reygers [102], V. Riabov [96], T. Richert [80,88], M. Richter [21], P. Riedler [34], W. Riegler [34], F. Riggi [28], C. Ristea [68], S.P. Rode [49], M. Rodríguez Cahuantzi [44], K. Røed [21], R. Rogalev [90], E. Rogochaya [75], D. Rohr [34], D. Röhrich [22], P.S. Rokita [142], F. Ronchetti [51], E.D. Rosas [70], K. Roslon [142], P. Rosnet [134], A. Rossi [29], A. Rotondi [139], F. Roukoutakis [83], A. Roy [49], P. Roy [108], O.V. Rueda [80], R. Rui [25], B. Rumyantsev [75], A. Rustamov [86], E. Ryabinkin [87], Y. Ryabov [96], A. Rybicki [118], H. Rytkonen [127], S. Saarinen [43], S. Sadhu [141], S. Sadovsky [90], K. Šafařík [37,34], S.K. Saha [141], B. Sahoo [48], P. Sahoo [49], R. Sahoo [49], S. Sahoo [66], P.K. Sahu [66], J. Saini [141], S. Sakai [133], S. Sambyal [99], V. Samsonov [96,91], A. Sandoval [72], A. Sarkar [73], D. Sarkar [141,143], N. Sarkar [141], P. Sarma [41], V.M. Sarti [103], M.H.P. Sas [63], E. Scapparone [53], B. Schaefer [94], J. Schambach [119], H.S. Scheid [69], C. Schiaua [47], R. Schicker [102], A. Schmah [102], C. Schmidt [105], H.R. Schmidt [101], M.O. Schmidt [102], M. Schmidt [101], N.V. Schmidt [94,69], A.R. Schmier [130], J. Schukraft [34,88], Y. Schutz [34,136], K. Schwarz [105], K. Schweda [105], G. Scioli [27], E. Scomparin [58], M. Šefčík [38], J.E. Seger [16], Y. Sekiguchi [132], D. Sekihata [45], I. Selyuzhenkov [105,91], S. Senyukov [136], D. Serebryakov [62], E. Serradilla [72], P. Sett [48], A. Sevcenco [68], A. Shabanov [62], A. Shabetai [114], R. Shahoyan [34], W. Shaikh [108], A. Shangaraev [90], A. Sharma [98], A. Sharma [99], M. Sharma [99], N. Sharma [98], A.I. Sheikh [141], K. Shigaki [45], M. Shimomura [82], S. Shirinkin [64], Q. Shou [111], Y. Sibiriak [87], S. Siddhanta [54], T. Siemiarczuk [84], D. Silvermyr [80], G. Simatovic [89], G. Simonetti [103,34], R. Singh [85], R. Singh [99], V.K. Singh [141], V. Singhal [141], T. Sinha [108], B. Sitar [14], M. Sitta [32], T.B. Skaali [21], M. Slupecki [127], N. Smirnov [146], R.J.M. Snellings [63], T.W. Snellman [127], J. Sochan [116], C. Soncco [110], J. Song [60,126], A. Songmoolnak [115], F. Soramel [29], S. Sorensen [130], I. Sputowska [118], J. Stachel [102], I. Stan [68], P. Stankus [94], P.J. Steffanic [130], E. Stenlund [80], D. Stocco [114], M.M. Storetvedt [36], P. Strmen [14], A.A.P. Suaide [121], T. Sugitate [45], C. Suire [61], M. Suleymanov [15], M. Suljic [34], R. Sultanov [64], M. Šumbera [93], S. Sumowidagdo [50], K. Suzuki [113], S. Swain [66], A. Szabo [14], I. Szarka [14], U. Tabassam [15], G. Taillepied [134],

J. Takahashi [122], G.J. Tambave [22], S. Tang [134,6], M. Tarhini [114], M.G. Tarzila [47], A. Tauro [34], G. Tejeda Muñoz [44], A. Telesca [34], C. Terrevoli [126,29], D. Thakur [49], S. Thakur [141], D. Thomas [119], F. Thoresen [88], R. Tieulent [135], A. Tikhonov [62], A.R. Timmins [126], A. Toia [69], N. Topilskaya [62], M. Toppi [51], F. Torales-Acosta [20], S.R. Torres [120], S. Tripathy [49], T. Tripathy [48], S. Trogolo [26,29], G. Trombetta [33], L. Tropp [38], V. Trubnikov [2], W.H. Trzaska [127], T.P. Trzcinski [142], B.A. Trzeciak [63], T. Tsuji [132], A. Tumkin [107], R. Turrisi [56], T.S. Tveter [21], K. Ullaland [22], E.N. Umaka [126], A. Uras [135], G.L. Usai [24], A. Utrobicic [97], M. Vala [116,38], N. Valle [139], S. Vallero [58], N. van der Kolk [63], L.V.R. van Doremalen [63], M. van Leeuwen [63], P. Vande Vyvre [34], D. Varga [145], M. Varga-Kofarago [145], A. Vargas [44], M. Vargyas [127], R. Varma [48], M. Vasileiou [83], A. Vasiliev [87], O. Vázquez Doce [117,103], V. Vechernin [112], A.M. Veen [63], E. Vercellin [26], S. Vergara Limón [44], L. Vermunt [63], R. Vernet [7], R. Vértesi [145], L. Vickovic [35], J. Viinikainen [127], Z. Vilakazi [131], O. Villalobos Baillie [109], A. Villatoro Tello [44], G. Vino [52], A. Vinogradov [87], T. Virgili [30], V. Vislavicius [88], A. Vodopyanov [75], B. Volkel [34], M.A. Völkl [101], K. Voloshin [64], S.A. Voloshin [143], G. Volpe [33], B. von Haller [34], I. Vorobyev [103,117], D. Voscek [116], J. Vrláková [38], B. Wagner [22], Y. Watanabe [133], M. Weber [113], S.G. Weber [105], A. Wegrzynek [34], D.F. Weiser [102], S.C. Wenzel [34], J.P. Wessels [144], E. Widmann [113], J. Wiechula [69], J. Wikne [21], G. Wilk [84], J. Wilkinson [53], G.A. Willems [34], E. Willsher [109], B. Windelband [102], W.E. Witt [130], Y. Wu [129], R. Xu [6], S. Yalcin [77], K. Yamakawa [45], S. Yang [22], S. Yano [137], Z. Yin [6], H. Yokoyama [63], I.-K. Yoo [18], J.H. Yoon [60], S. Yuan [22], A. Yuncu [102], V. Yurchenko [2], V. Zaccolo [58,25], A. Zaman [15], C. Zampolli [34], H.J.C. Zanoli [121], N. Zardoshti [34], A. Zarochentsev [112], P. Závada [67], N. Zaviyalov [107], H. Zbroszczyk [142], M. Zhalov [96], X. Zhang [6], Z. Zhang [6,134], C. Zhao [21], V. Zherebchevskii [112], N. Zhigareva [64], D. Zhou [6], Y. Zhou [88], Z. Zhou [22], J. Zhu [6], Y. Zhu [6], A. Zichichi [27,10], M.B. Zimmermann [34], G. Zinovjev [2], N. Zurlo [140]

[1] *A.I. Alikhanyan National Science Laboratory (Yerevan Physics Institute) Foundation, Yerevan, Armenia*
[2] *Bogolyubov Institute for Theoretical Physics, National Academy of Sciences of Ukraine, Kiev, Ukraine*
[3] *Bose Institute, Department of Physics and Centre for Astroparticle Physics and Space Science (CAPSS), Kolkata, India*
[4] *Budker Institute for Nuclear Physics, Novosibirsk, Russia*
[5] *California Polytechnic State University, San Luis Obispo, CA, United States*
[6] *Central China Normal University, Wuhan, China*
[7] *Centre de Calcul de l'IN2P3, Villeurbanne, Lyon, France*
[8] *Centro de Aplicaciones Tecnológicas y Desarrollo Nuclear (CEADEN), Havana, Cuba*
[9] *Centro de Investigación y de Estudios Avanzados (CINVESTAV), Mexico City and Mérida, Mexico*
[10] *Centro Fermi - Museo Storico della Fisica e Centro Studi e Ricerche 'Enrico Fermi', Rome, Italy*
[11] *Chicago State University, Chicago, IL, United States*
[12] *China Institute of Atomic Energy, Beijing, China*
[13] *Chonbuk National University, Jeonju, Republic of Korea*
[14] *Comenius University Bratislava, Faculty of Mathematics, Physics and Informatics, Bratislava, Slovakia*
[15] *COMSATS University Islamabad, Islamabad, Pakistan*
[16] *Creighton University, Omaha, NE, United States*
[17] *Department of Physics, Aligarh Muslim University, Aligarh, India*
[18] *Department of Physics, Pusan National University, Pusan, Republic of Korea*
[19] *Department of Physics, Sejong University, Seoul, Republic of Korea*
[20] *Department of Physics, University of California, Berkeley, CA, United States*
[21] *Department of Physics, University of Oslo, Oslo, Norway*
[22] *Department of Physics and Technology, University of Bergen, Bergen, Norway*
[23] *Dipartimento di Fisica dell'Università 'La Sapienza' and Sezione INFN, Rome, Italy*
[24] *Dipartimento di Fisica dell'Università and Sezione INFN, Cagliari, Italy*
[25] *Dipartimento di Fisica dell'Università and Sezione INFN, Trieste, Italy*
[26] *Dipartimento di Fisica dell'Università and Sezione INFN, Turin, Italy*
[27] *Dipartimento di Fisica e Astronomia dell'Università and Sezione INFN, Bologna, Italy*
[28] *Dipartimento di Fisica e Astronomia dell'Università and Sezione INFN, Catania, Italy*
[29] *Dipartimento di Fisica e Astronomia dell'Università and Sezione INFN, Padova, Italy*
[30] *Dipartimento di Fisica 'E.R. Caianiello' dell'Università and Gruppo Collegato INFN, Salerno, Italy*
[31] *Dipartimento DISAT del Politecnico and Sezione INFN, Turin, Italy*
[32] *Dipartimento di Scienze e Innovazione Tecnologica dell'Università del Piemonte Orientale and INFN Sezione di Torino, Alessandria, Italy*
[33] *Dipartimento Interateneo di Fisica 'M. Merlin' and Sezione INFN, Bari, Italy*
[34] *European Organization for Nuclear Research (CERN), Geneva, Switzerland*
[35] *Faculty of Electrical Engineering, Mechanical Engineering and Naval Architecture, University of Split, Split, Croatia*
[36] *Faculty of Engineering and Science, Western Norway University of Applied Sciences, Bergen, Norway*
[37] *Faculty of Nuclear Sciences and Physical Engineering, Czech Technical University in Prague, Prague, Czech Republic*
[38] *Faculty of Science, P.J. Šafárik University, Košice, Slovakia*
[39] *Frankfurt Institute for Advanced Studies, Johann Wolfgang Goethe-Universität Frankfurt, Frankfurt, Germany*
[40] *Gangneung-Wonju National University, Gangneung, Republic of Korea*
[41] *Gauhati University, Department of Physics, Guwahati, India*
[42] *Helmholtz-Institut für Strahlen- und Kernphysik, Rheinische Friedrich-Wilhelms-Universität Bonn, Bonn, Germany*
[43] *Helsinki Institute of Physics (HIP), Helsinki, Finland*
[44] *High Energy Physics Group, Universidad Autónoma de Puebla, Puebla, Mexico*
[45] *Hiroshima University, Hiroshima, Japan*
[46] *Hochschule Worms, Zentrum für Technologietransfer und Telekommunikation (ZTT), Worms, Germany*

[47] Horia Hulubei National Institute of Physics and Nuclear Engineering, Bucharest, Romania
[48] Indian Institute of Technology Bombay (IIT), Mumbai, India
[49] Indian Institute of Technology Indore, Indore, India
[50] Indonesian Institute of Sciences, Jakarta, Indonesia
[51] INFN, Laboratori Nazionali di Frascati, Frascati, Italy
[52] INFN, Sezione di Bari, Bari, Italy
[53] INFN, Sezione di Bologna, Bologna, Italy
[54] INFN, Sezione di Cagliari, Cagliari, Italy
[55] INFN, Sezione di Catania, Catania, Italy
[56] INFN, Sezione di Padova, Padova, Italy
[57] INFN, Sezione di Roma, Rome, Italy
[58] INFN, Sezione di Torino, Turin, Italy
[59] INFN, Sezione di Trieste, Trieste, Italy
[60] Inha University, Incheon, Republic of Korea
[61] Institut de Physique Nucléaire d'Orsay (IPNO), Institut National de Physique Nucléaire et de Physique des Particules (IN2P3/CNRS), Université de Paris-Sud, Université Paris-Saclay, Orsay, France
[62] Institute for Nuclear Research, Academy of Sciences, Moscow, Russia
[63] Institute for Subatomic Physics, Utrecht University/Nikhef, Utrecht, Netherlands
[64] Institute for Theoretical and Experimental Physics, Moscow, Russia
[65] Institute of Experimental Physics, Slovak Academy of Sciences, Košice, Slovakia
[66] Institute of Physics, Homi Bhabha National Institute, Bhubaneswar, India
[67] Institute of Physics of the Czech Academy of Sciences, Prague, Czech Republic
[68] Institute of Space Science (ISS), Bucharest, Romania
[69] Institut für Kernphysik, Johann Wolfgang Goethe-Universität Frankfurt, Frankfurt, Germany
[70] Instituto de Ciencias Nucleares, Universidad Nacional Autónoma de México, Mexico City, Mexico
[71] Instituto de Física, Universidade Federal do Rio Grande do Sul (UFRGS), Porto Alegre, Brazil
[72] Instituto de Física, Universidad Nacional Autónoma de México, Mexico City, Mexico
[73] iThemba LABS, National Research Foundation, Somerset West, South Africa
[74] Johann-Wolfgang-Goethe Universität Frankfurt Institut für Informatik, Fachbereich Informatik und Mathematik, Frankfurt, Germany
[75] Joint Institute for Nuclear Research (JINR), Dubna, Russia
[76] Korea Institute of Science and Technology Information, Daejeon, Republic of Korea
[77] KTO Karatay University, Konya, Turkey
[78] Laboratoire de Physique Subatomique et de Cosmologie, Université Grenoble-Alpes, CNRS-IN2P3, Grenoble, France
[79] Lawrence Berkeley National Laboratory, Berkeley, CA, United States
[80] Lund University Department of Physics, Division of Particle Physics, Lund, Sweden
[81] Nagasaki Institute of Applied Science, Nagasaki, Japan
[82] Nara Women's University (NWU), Nara, Japan
[83] National and Kapodistrian University of Athens, School of Science, Department of Physics, Athens, Greece
[84] National Centre for Nuclear Research, Warsaw, Poland
[85] National Institute of Science Education and Research, Homi Bhabha National Institute, Jatni, India
[86] National Nuclear Research Center, Baku, Azerbaijan
[87] National Research Centre Kurchatov Institute, Moscow, Russia
[88] Niels Bohr Institute, University of Copenhagen, Copenhagen, Denmark
[89] Nikhef, National Institute for Subatomic Physics, Amsterdam, Netherlands
[90] NRC Kurchatov Institute IHEP, Protvino, Russia
[91] NRNU Moscow Engineering Physics Institute, Moscow, Russia
[92] Nuclear Physics Group, STFC Daresbury Laboratory, Daresbury, United Kingdom
[93] Nuclear Physics Institute of the Czech Academy of Sciences, Řež u Prahy, Czech Republic
[94] Oak Ridge National Laboratory, Oak Ridge, TN, United States
[95] Ohio State University, Columbus, OH, United States
[96] Petersburg Nuclear Physics Institute, Gatchina, Russia
[97] Physics Department, Faculty of Science, University of Zagreb, Zagreb, Croatia
[98] Physics Department, Panjab University, Chandigarh, India
[99] Physics Department, University of Jammu, Jammu, India
[100] Physics Department, University of Rajasthan, Jaipur, India
[101] Physikalisches Institut, Eberhard-Karls-Universität Tübingen, Tübingen, Germany
[102] Physikalisches Institut, Ruprecht-Karls-Universität Heidelberg, Heidelberg, Germany
[103] Physik Department, Technische Universität München, Munich, Germany
[104] Politecnico di Bari, Bari, Italy
[105] Research Division and ExtreMe Matter Institute EMMI, GSI Helmholtzzentrum für Schwerionenforschung GmbH, Darmstadt, Germany
[106] Rudjer Bošković Institute, Zagreb, Croatia
[107] Russian Federal Nuclear Center (VNIIEF), Sarov, Russia
[108] Saha Institute of Nuclear Physics, Homi Bhabha National Institute, Kolkata, India
[109] School of Physics and Astronomy, University of Birmingham, Birmingham, United Kingdom
[110] Sección Física, Departamento de Ciencias, Pontificia Universidad Católica del Perú, Lima, Peru
[111] Shanghai Institute of Applied Physics, Shanghai, China
[112] St. Petersburg State University, St. Petersburg, Russia
[113] Stefan Meyer Institut für Subatomare Physik (SMI), Vienna, Austria
[114] SUBATECH, IMT Atlantique, Université de Nantes, CNRS-IN2P3, Nantes, France
[115] Suranaree University of Technology, Nakhon Ratchasima, Thailand
[116] Technical University of Košice, Košice, Slovakia
[117] Technische Universität München, Excellence Cluster 'Universe', Munich, Germany
[118] The Henryk Niewodniczanski Institute of Nuclear Physics, Polish Academy of Sciences, Cracow, Poland
[119] The University of Texas at Austin, Austin, TX, United States
[120] Universidad Autónoma de Sinaloa, Culiacán, Mexico
[121] Universidade de São Paulo (USP), São Paulo, Brazil
[122] Universidade Estadual de Campinas (UNICAMP), Campinas, Brazil
[123] Universidade Federal do ABC, Santo Andre, Brazil
[124] University College of Southeast Norway, Tonsberg, Norway

[125] University of Cape Town, Cape Town, South Africa
[126] University of Houston, Houston, TX, United States
[127] University of Jyväskylä, Jyväskylä, Finland
[128] University of Liverpool, Liverpool, United Kingdom
[129] University of Science and Techonology of China, Hefei, China
[130] University of Tennessee, Knoxville, TN, United States
[131] University of the Witwatersrand, Johannesburg, South Africa
[132] University of Tokyo, Tokyo, Japan
[133] University of Tsukuba, Tsukuba, Japan
[134] Université Clermont Auvergne, CNRS/IN2P3, LPC, Clermont-Ferrand, France
[135] Université de Lyon, Université Lyon 1, CNRS/IN2P3, IPN-Lyon, Villeurbanne, Lyon, France
[136] Université de Strasbourg, CNRS, IPHC UMR 7178, F-67000 Strasbourg, France
[137] Université Paris-Saclay Centre d'Etudes de Saclay (CEA), IRFU, Département de Physique Nucléaire (DPhN), Saclay, France
[138] Università degli Studi di Foggia, Foggia, Italy
[139] Università degli Studi di Pavia, Pavia, Italy
[140] Università di Brescia, Brescia, Italy
[141] Variable Energy Cyclotron Centre, Homi Bhabha National Institute, Kolkata, India
[142] Warsaw University of Technology, Warsaw, Poland
[143] Wayne State University, Detroit, MI, United States
[144] Westfälische Wilhelms-Universität Münster, Institut für Kernphysik, Münster, Germany
[145] Wigner Research Centre for Physics, Hungarian Academy of Sciences, Budapest, Hungary
[146] Yale University, New Haven, CT, United States
[147] Yonsei University, Seoul, Republic of Korea

[i] Deceased.
[ii] Dipartimento DET del Politecnico di Torino, Turin, Italy.
[iii] M.V. Lomonosov Moscow State University, D.V. Skobeltsyn Institute of Nuclear Physics, Moscow, Russia.
[iv] Department of Applied Physics, Aligarh Muslim University, Aligarh, India.
[v] Institute of Theoretical Physics, University of Wroclaw, Poland.